Isolation of cancer cells on nanomaterial functionalized microfluidic devices

Bhuwan Ghimire

Supervisors: Dr. Lianmei Jiang and Prof. Jim Piper

A thesis submitted to Macquarie University

for the degree of Master of Research

Department of Physics

October 2018

MACQUARIE
University

Statement of originality

This thesis to the best of my knowledge does not contain any material that has been accepted for any other degree in any institution and does not have any materials published anywhere else, except where due references have been made within the thesis. The contributions of others efforts have been duly acknowledged.

Bhuwan Ghimire

Acknowledgements

Firstly, I wish to express my sincere thanks to Prof. Jim Piper for providing me the opportunity to work on this project and my supervisor Dr. Lianmei Jiang who gave me complete freedom to pursue my ideas throughout this project. This thesis would not be possible without both of their guidance, support and ideas.

Big thanks to Dr. Nima Sayyadi, for his efficient and supportive nature throughout this time for the successful completion of this project and to Victoria Wang for the cell cultures used for this project.

Thanks to members of BMMD group and CNBP for their suggestions during the project.

I also wish to acknowledge the ARC Centre of Excellence for Nanoscale Biophotonics and Macquarie University for funding the research and scholarship components of this project respectively.

Abstract

Primary cancerous tumors release cells that either stay locally or metastasize (spread) to different tissues through blood, referred to as circulating tumor cells (CTCs). CTCs are extremely rare in patients with metastatic cancer in initial stages (one cell per 10^9 hematologic cells in blood approx.) Isolation of circulating tumor cells (CTCs) is widely pursued as these cells provide valuable information about the metastasis and invasiveness of cancer growth through protein expression and is a critical element for therapeutic monitoring. Conventional batch processing methods do not provide precise safe handling and spatial-temporal manipulation for CTCs. Enrichment of CTCs with microfluidic methods provides a non-surgical, non-invasive and cost-effective alternative for CTC isolation through analysis of body fluids like blood or urine in case of bladder cancer. This thesis presents the fabrication, optimization and capture analysis results of a microfluidic device developed for capturing DU145, a prostate cancer cell line. Potential of the nanomaterial graphene oxide has been investigated in capture of these cells via immuno-affinity binding with the MIL-38 antibody inside the device. Binding affinity of antibodies towards the functionalized surfaces has been explored. The capture rates for DU145 and C3 cell lines on graphene oxide functionalized and non-functionalized surfaces are presented in this thesis.

Table of Contents

List of Figures

Chapter 1

Chapter 2

Chapter 3

Chapter 4

Chapter 1.

Introduction

1.1 Introduction to the thesis

Cancer cells can migrate from their primary growth site to secondary sites through a bioprocess known as metastasis[1,2]. These metastasizing cells, termed circulating tumor cells (CTCs), circulate to distant sites where they make new colonies and may infect local cells[3,4]. Circulating tumor cells can provide valuable information regarding the stages of cancer, antigen expressions and can be used as biomarkers in detection and therapeutic monitoring. Prognostic value of CTC enumeration in cancer cell lines of prostate, breast, lung and colorectal cancer have been reviewed[5-9]. Although the value of CTCs as biomarkers is undisputed, the rarity of these cells (1 in 10^9 hematologic cells approx.) makes the isolation and detection of them challenging in early stages of cancer. Research on circulating tumor cells and metastasis currently focuses on enrichment of these cells and potential therapeutic monitoring[10].

Conventional methods in CTC isolation and detection use surgical biopsies transplanted to mouse models. Though these are frequently employed by tumor clinicians, these methods are invasive processes both for the patients and the cell samples specimens. Liquid biopsies like blood and urine present a much less invasive and faster method of tumor cells isolation, enrichment and detection. Flow cytometry and DNA sequencing techniques are quite expensive and time-consuming procedures for cancer detection. Microfluidic assay-based isolation of CTCs provides a faster, cheaper and more efficient approach to direct detection of biomarkers in fluid samples. With its ability to manipulate microliter volumes of fluid specimens at fast processing rates, microfluidics technology provides unrivalled advantages in volume consumption of costly bio functionalization materials, is less invasive for tumor cell samples extraction from patients and provides further direct detection platforms.

Nanomaterials in microfluidic platforms have been recently used to maximize surface area for detection of biomolecules by functionalization of the devices[11-13]. For this project, we have designed microfluidic devices with nanomaterial (Graphene oxide) modified surfaces for microfluidic devices for efficient capture of DU145 cells (a prostate cancer cell line) using C3 cells as the negative control line. We used chaotic mixing technology for maximum interaction of biomarker targets and capture bioreceptors. We compared and contrasted the binding affinities of capture antibodies towards the Graphene Oxide (GO) functionalized substrates vs non-functionalized substrates.

The project in its entirety was conducted within the Australian Research Council (ARC) Centre of Excellence for Nanoscale Biophotonics (CNBP) and the Department of Physics and Astronomy at Macquarie University in Sydney, Australia. The research component of this project was funded by the ARC-CBP grant number CE140100003 and the candidate's scholarship was funded by Macquarie university. The initial master mold design for the microfluidic channels was provided by Dr. Lianmei Jiang and Yan Wang provided the DU145 and C3 cells used for this project.

The thesis format follows the University's Faculty of Science's guidelines including the maximum pages allowed and the results presented are for the Master of Research (MRes) project conducted between January-September 2018. The thesis consists of 4 chapters:

Chapter 1 presents the introduction of the thesis and the motivation of the research. It discusses a brief background on circulating tumor cells, advantages and applications of microfluidics in isolating and detecting CTCs and the role of nanomaterials in surface functionalization on microfluidic devices.

Chapter 2 details our approach to the research, the experimental methods and discusses the materials, analytical tools and instrumentation used.

Chapter 3 presents our approach to graphene oxide functionalization in glass substrates and the results of binding affinities of antibodies and cell capture efficiency in our devices.

Chapter 4 summarizes the conclusions of our work and closes the thesis with the future approach and perspectives for this project.

The results of this project have been presented in:

- *"A microfluidic device for capture and detection of circulating tumor cells"*, Bhuwan Ghimire, Lianmei Jiang, Jim Piper., Australia and New Zealand Nano and Microfluidics (ANZNMF), Vol 9 | 27 - 29 June, 2018

1.2 Circulating tumor cells

A cancerous tumor can contain millions or billions of cells that can harbor mutations, which allows them to grow uncontrollably (mutate) and attack the local cells[3,4,14]. For most types of cancer, primary tumors release cells that either stay locally (self-seeding) or move out to adjacent tissues- a process called as metastasis[1,2]. These metastasizing cells so-called circulating tumor cells (CTCs) circulate to distant sites where they make new colonies. Among cancer related deaths, metastatic diseases are found to be responsible for 90% of the cases[15-17].

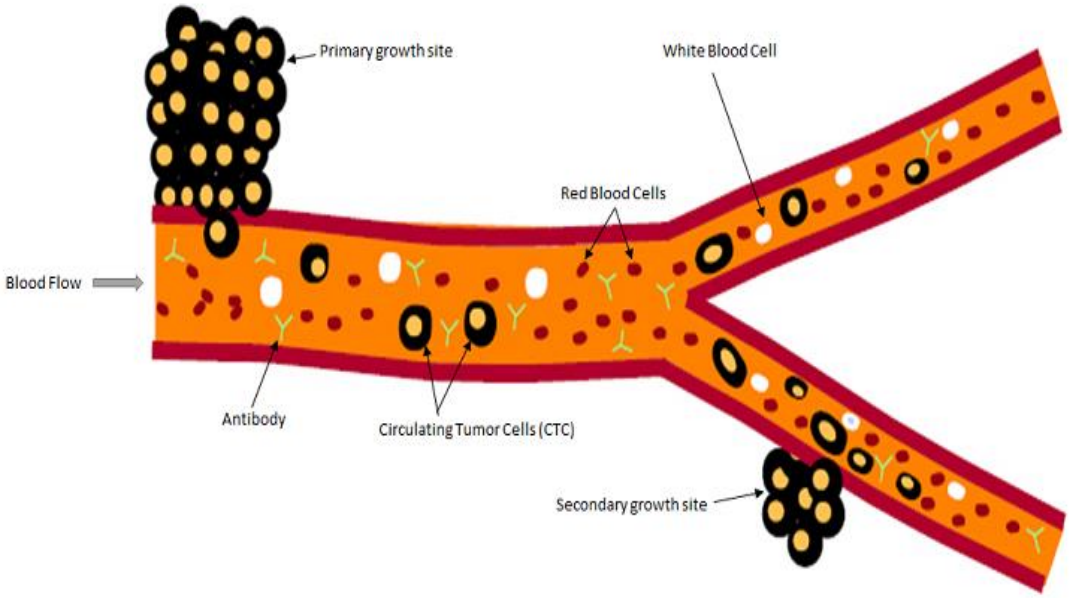

Figure 1. Illustration of circulating tumor Cells (CTC) undergoing metastasis from a primary growth side to a secondary growth site via circulation through bloodstream.

The idea that circulating tumor cells were a necessary element towards metastasis or the growth of secondary tumor site from a primary site was proposed in the 19th century by the pathologist Thomas Ashworth who reported a case of cancer where cells similar to those found in tumors as being present in blood after death[5]. Research in levels of CTCs in metastatic cancer patients has shown its value as a biomarker in detection and treatment procedures. The prognostic value of CTC enumeration in cancer cell lines of prostate, breast, lung and colorectal cancer has been reviewed[5-9]. The identification and characterization of CTCs is key to insights into cancer metastasis and expected to reveal novel targets for cancer detection and therapeutic monitoring. CTCs can be captured with non-invasive methods from a patient's liquid biopsy (i.e. blood, urine.) that does not require the collection of a tumor specimen (surgical biopsy) from the patient. Thus, technologies that can trap, detect and characterize CTCs directly from patient's blood and urine samples are highly sought in cancer detection[7,18-23].

1.2.1 Methods for CTC isolation

Circulating tumor cells are isolated with a wide variety of techniques including batch processes; affinity based and label free technologies like electrophoresis and acoustophoresis[11,24,25]. For this thesis, we discuss only the technologies using microfluidic based platforms for capture and characterization that combines both distinctive biophysical and biochemical properties of CTCs. Listed below are the major techniques employing microfluidic platforms for isolating CTCs:

a. Affinity based isolation

This is one of the most widely used technique for isolating CTCs in microfluidic devices[11,13,26-28]. This technique uses affinity of antigens expressed by CTCs towards binding sites presented by the surface of the antibodies. This technique is integrated commonly with other label free techniques for isolation of CTCs. Enrichment of cells are achieved with this approach in both positive and negative ways. Nagrath et al. (2014) used a radial structured chip that introduced a varying shear flow profile enabling direct cell capture by positive affinity at high flow rates[24]. Jung et al. used a geometrically activated surface interaction (GASI) chip with an asymmetric herringbone structure to increase the surface interaction between the non-target cells and the channel surface[27]. In this case, non-target cells were isolated and target cells were released for collection.

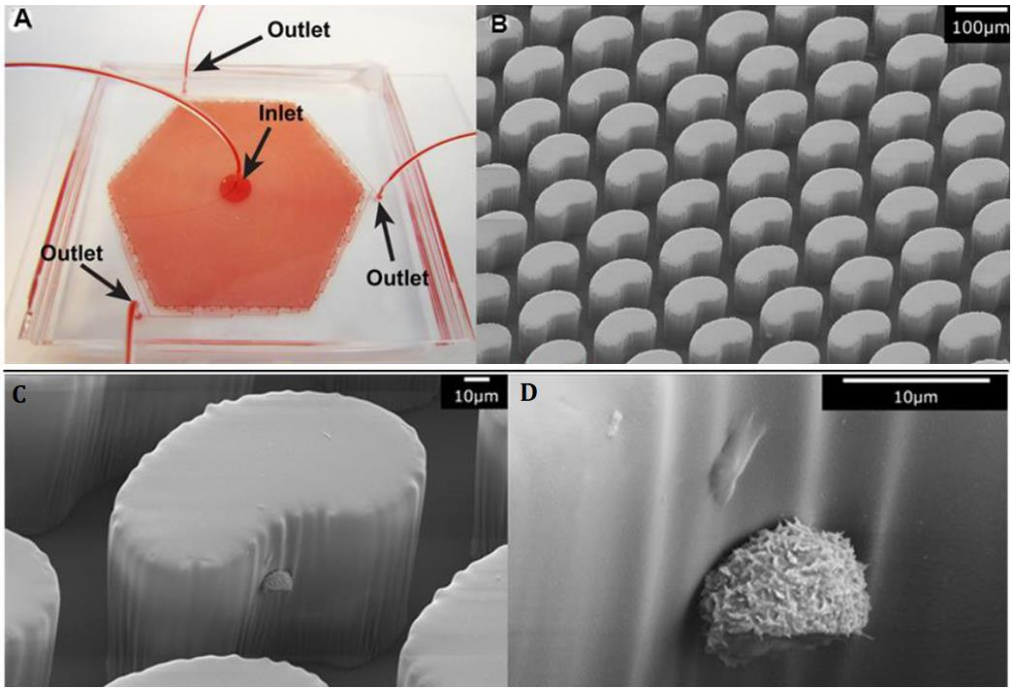

Figure 2. The OncoBean Chip by Nagrath et al. (2014) using immunoaffinity with bean structures to capture CTCs. (A) Top view of the OncoBean chip (B) SEM image of the bean shaped micro structures of the device. (C) SEM image of a H1650 cell captured on a bean shaped structure and (H) Magnified SEM image.

b. Physical properties based:

These techniques are label free methods that use the physical characteristics of cells[29] as well as the application of external physical forces like di-electrophoresis and acoustophoresis phenomena to sort and isolate CTCs[20,30-32]. As cancer cells are generally larger in size than normal cells, some methods use filtration tools like pores and micro filters to first sort CTCs[29,33] from non-target cells and dust and further capture these CTCs in a container outside of the chip. Yasuda et al. (2004) used a PDMS based micro array filter (Fig.3) to remove dust from their sample as a pre-processing unit[34]. Krebs et al. used the ISET filtration technology of RareCell Diagnostics to isolate CTCs independent of their biomarker expression using the ISET filter module of a polycarbonate track-etched-type membrane that contained pierced 8µm cylindrical pores[33]. This filtration technique is only helpful for enrichment outside the device by sorting cells according to their size and can have impurity issues.

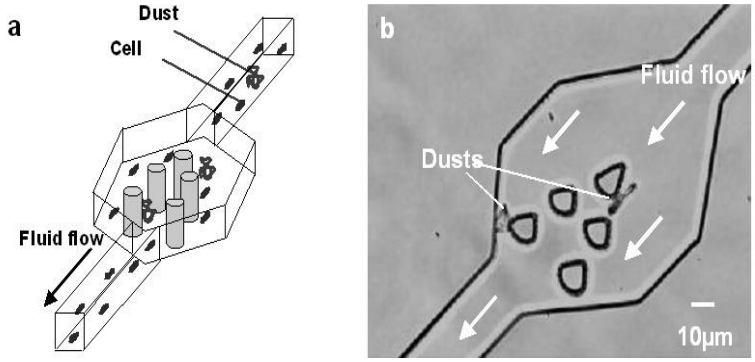

Figure 3. A micro- filter system chip developed by Yasuda et al. (2004)[34]. (a) Schematic view of the filters (b) Optical micrograph of the filter used in the micro filter system.

The application of external physical forces including di-electrophoresis, magnetophoresis and acoustophoresis phenomena are used to sort and isolate CTCs through this method[20,30-32]. These techniques do not require affinity-based properties of CTCs and depend on the dielectric properties of the cell as well as on the use acoustic forces. These can be integrated with the above-mentioned affinity-based methods for enhanced sorting inside the device chip and capture of CTCs outside the device. These do not provide localized isolation or capture within the devices and are more of a sorting technique. These are not relevant to the thesis work and we will not discuss this in detail further in this thesis.

1.2.2 Methods for CTC detection

After isolation or sorting of CTCs, detection is the next step. Novel CTC detection technologies have existed for the past two decades [7,23,35]. They primarily fall into two categories:

i. Nucleic acid-based techniques: These methods were developed using Polymerase chain reaction (PCR), which may detect specific DNA or RNA sequences expressed by tumour cells. The scope and examples of nucleic acids can be vast, but this technique is not part of this project and we will not discuss this further for this review.

ii. Cytometric based approaches: Cytometry is the measurement of cell characteristics including cell size, cell count, cell morphology, cell antigens and expression of proteins in the cell surface. Several cytometric devices exist including flow cytometers, image cytometers and cell sorters. These methods commonly use immunostaining to detect CTCs. Among these techniques, image cytometers commonly employ fluorochrome labelling of cells as a detection technique and immunoaffinity as an analysis technique. Prior to detection, a pre-enrichment step using isolation techniques is necessary. Recently developed CTC isolation methods use antibodies that bind to epithelial cell-adhesion molecule (EpCAM), a protein which is present on the outer surface of CTCs and non-healthy blood cells[14]. Final detection of cells is then achieved by fluorescence microscopy and immunohistochemistry. CellSearch™ platform, which uses an immunomagnetic approach to capture CTCs, is one of the most used cytometric CTC technologies[19] that performs enumeration of CTCs in whole blood of cancer patients. To date, it remains the only US Food and Drug Administration (FDA) approved technology for clinical use to detect CTCs in blood. Many recent platforms employ microfluidics as the primary isolation tool for the enumeration and on chip detection of CTCs[12,23,36,37] . Researchers have also combined novel technologies in photonics such as time-gated luminescence and immune-affinity to detect cancer cells through chemical ligands[38].

   We have combined microfluidics and nanomaterials functionalization for CTC isolation and capture for further detection using fluorescence microscopy.

1.3 Introduction to Microfluidics and its overall advantages

Microfluidics is the manipulation and processing of fluids on the microscale using channels of dimensions of tens to hundreds of micrometres. At this scale, the effect of inertial forces (fluid velocity, gravity) are negligible on fluids and viscous forces (viscosity) dominate the flow profiles.

The result is laminar flow where fluids co-flow and there is no convective mixing[39]. Molecular transport can thus only occur through diffusion. A user employing microfluidic platforms for their experiments can thus take the advantage of uniform and stable reaction conditions with laminar flow. Early research in microfluidics was limited to theoretical studies of fluid dynamics at the microscale. A keyword search of 'Microfluidics' through google scholar until 1970 reports just under 80 results of which the majority are patents. However, the expiry of key patents during the end of the 20th century and early 21st century have allowed this technique to revolutionize many other scientific areas.

Before the advent of applied microfluidics, much of the experimental research in cellular biology and medicine was performed with batch processing and macro experiments that employed conventional flasks and petri-dish based methods. These methods were not only time consuming but also required excess resources, manpower and included the risk of contamination during experiments. These techniques have been slowly substituted by microfluidic based techniques that provide an unrivalled tool to significantly reduce the costs and time required for biological research significantly. Microfluidics offers the tools to create confined microenvironments on a cellular scale that would otherwise not be possible with batch processing methods. This initiates a much better space-time control of parameters critical in experimental research in biology and medicine.

Today, microfluidics has metamorphosed from a purely theoretical research topic into a field influencing global research areas covering cellular biology, nanotechnology, materials science, medical diagnostics, environmental science and global health. In the past two decades, there have been numerous applications of microfluidics science due to its advantages of low analytes volume consumption, low cost, high sensitivity and detection in analytical sciences. George M. Whitesides predicted in his article 'The origins and the future of microfluidics' in Nature (2006) that "microfluidic technology will become a major theme in the analysis, and perhaps synthesis of molecules: the advantages it offers are too compelling to let pass"[40]. The predictions have been met, as Elveflow through google scholar reported in 2015 that there has been 10 times more publications on microfluidics and biology since 2002[41].

1.4 Theoretical Overview and Concept of Micro Flows in microfluidics

A sound understanding of fluid dynamics and theoretical concepts of flows at the microscale is necessary to master the technology of microfluidics experimentally. Fluid flows in microscale is laminar (Low Reynolds number) and biological fluids can have different viscosities. It is essential to understand the basic concepts of fluid dynamics to control flow rates, pressure drops, and analytes interactions between microchannels depending on the experiments.

Sir Issac Newton (1624-1726) used the flow behaviour of fluids to derive a linear relation between shear stress and shear rate. This led to Newton's law of viscosity for the Newtonian fluids named after him. It states that the shear stress between adjacent unidirectional fluid layers is proportional to the velocity gradients between two layers. The ratio of shear stress to shear rate is a constant, for a given temperature and pressure, and this is known as the 'viscosity' of the fluids. The equation is as follows:

$$\tau = \mu * \dot{\gamma} \tag{1}$$

where, τ is the shear stress, μ is the fluid viscosity, $\dot{\gamma}$ is the shear rate which is expressed as (v/h): the rate of velocity (v) over the distance (h) between two parallel plates, where one is moving at constant speed and the other is stationary.

Equation (1) is true for Newtonian fluids like water, urine and organic solvents. For these fluids, viscosity is dependent only on temperature. This is not applicable for non-Newtonian fluids like corn starch in water, nail polish, silicone oils etc. (Fig 4). However, these fluids are not applicable to this project and the theory of flow concepts for these fluids will not be discussed in this thesis. Blood samples are used for extraction of CTCs however these samples are diluted with water for infusion inside the microfluidic devices.

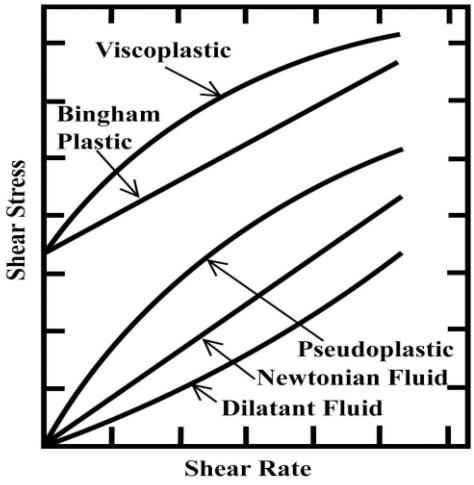

Figure 4. Qualitative flow curves for newtonian vs non-newtonian fluids[42].

To understand micro-flows and concept of laminarity in fluid dynamics, we have to understand Navier-stokes equations which govern flows. For a constant density and unidirectional fluid, the Navier-Stoke equation can be expressed as:

$$\rho\, \vec{g} - \nabla \vec{p} + \mu . \nabla^2 \vec{u} = \rho \left(\vec{u} . \nabla \vec{u} + \frac{\partial \vec{u}}{\partial t} \right) \tag{2}$$

In the equation above,

'ρ' is the density,

'$\vec{g}$' is the gravity,

'p' is the pressure,

'μ' is the viscosity,

$\vec{u}$ is the fluid velocity.

Reynolds number is the ratio of inertial forces to viscous forces. Reynolds number predicts whether the flow will be turbulent (> 4000) or laminar (< 2100). It is expressed as:

$$R_e = \frac{\rho u L}{\mu} = \frac{uL}{\nu} \tag{3}$$

where,

'ρ' is the density,

'ν' is the kinematic viscosity, which is ratio of dynamic viscosity μ to the density ρ of the fluid,

'u' is the velocity of the fluid with respect to an object,

'L' is the length scale in any system.

In the microfluidic realm, the value of the Reynolds number (R_e) can be calculated for a fluid like water (20ºC) in a channel of 100 microns height as:

$$R_e = \frac{\rho u L}{\mu} \approx \frac{1000*1*100.10^{-6}}{10^{-3}} \approx 10^2 \ll 2100 \tag{4}$$

This means the flow is laminar. As viscous forces dominate in laminar flows and inertial forces can be neglected, for an incompressible, steady and Newtonian micro-fluid, simplifications to the Navier Stokes equations (Eqn. 2) can be made by neglecting gravity, fluid velocity and the fluid inertia, so the Navier-Stokes equation can be simplified and rewritten as:

$$\nabla \vec{p} = \eta \nabla^2 \vec{u} \tag{5}$$

This equation shows that pressure forces balance the viscous forces in the microfluidic realm. This equation can be solved for various shaped micro-channels.

For a viscous fluid through a channel with a rectangular cross-section (the device used for this thesis has a similar cross section), the volumetric flow rate, Q, is similar to the Hagen-Poiseuille equation for laminar, viscous and incompressible flow [7]:

$$Q = \frac{W_c H_c^3}{12 \mu L_c} \Delta P, \tag{6}$$

where,

W_c,, H_c and L_c are the width, height and length of the channel respectively,

ΔP is the pressure drop along the length of the channel,
μ is the fluid viscosity,

The average flow rate of a fluid within a microfluidic channel is proportional to the pressure gradient on both ends of the channel. Thus, the Hagen-Poiseuille equation can be rewritten as a classical Ohm's law (analogous to the ratio of voltage to current through a resistor for electrical resistance) and is expressed as:

$$\Delta P = QR_c \tag{7}$$

The resistance calculations can be handy on channels where the channel aspect ratio is very high (i.e., the height is much smaller than the width). In that case as the height is much more influential in a microchannel (to the power 3) in equation 6, a smaller height would mean very high resistance and the pressure drop would be significant which would mean a much higher flow rate would be required to pump fluids in any microchannels.

As the Reynolds number is small in microfluidics, turbulence does not occur in microscale fluid dynamics and mixing depends on chaotic advection[43]. Mixing can be achieved with two different techniques, namely: active and passive mixing[44-46]. Active mixing includes active components like external pressure induced perturbations and actuators, acoustically driven flows and temperature induced mixing. This type of mixing is not the science of our microfluidic device and hence will not be discussed further in this thesis. Passive mixing relies on special channels, geometry of devices and microstructures inside the device like the herringbone mixer, 3D serpentine channels, hydrodynamic flow focuser and cross flow mixer to name a few. There are three nondimensional parameters that are considered important in micromixers: The Reynolds number (Re), Peclet number (Pe), and Strouhal number (St.). The Reynolds number has already been discussed before. Peclet number is relevant in the study of transport phenomena of molecules and is the ratio of advection and diffusion of a physical quantity by the flow. For mass transport, it is given by:

$$Pe = \frac{advective\ transport\ rate}{diffusive\ transport\ rate} = \frac{Lu}{D} = Re_L Sc$$

where, D is the mass diffusion coefficient, u is the local flow velocity and L is the characteristic length, Re is the Reynolds number and Sc is the Schmidt number.

The Strouhal number defines oscillating flow mechanisms[47,48] and is described as:

$$St = \frac{fL}{u},$$

where, f is the frequency of the vortex shedding and represents the ratio between residence time of a sample species and time period of disturbance, L is the characteristic length and u is the flow velocity.

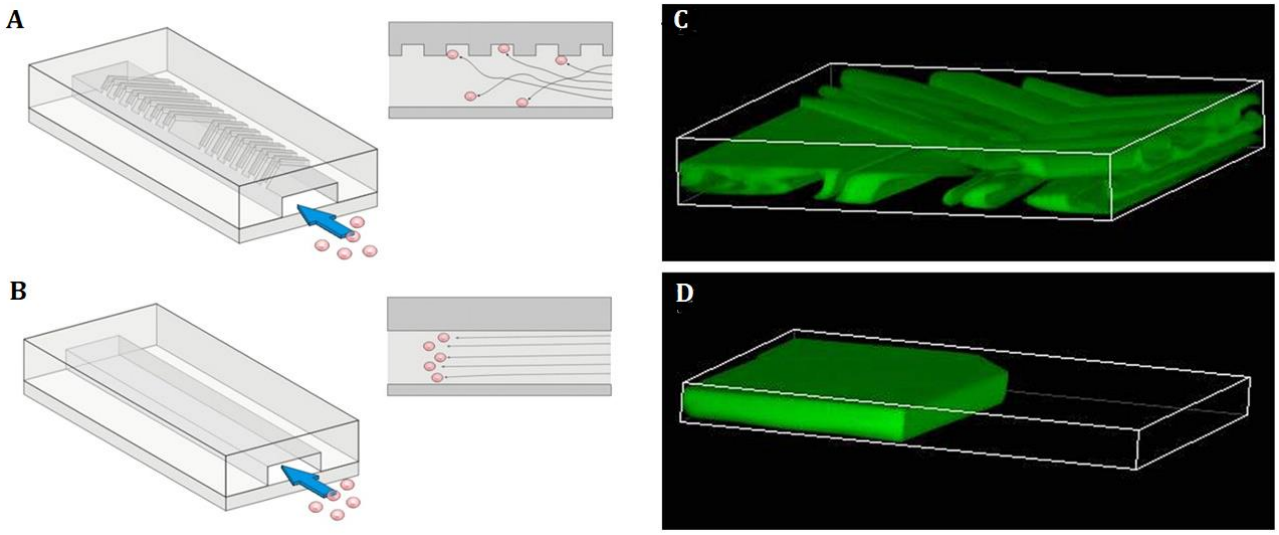

Figure 5. The Herringbone (HB) chip technique for maximum target-bioreceptor interaction for capturing CTCs by Stott et al. a) Schematic of the HB design with target and surface interaction, b) Schematic of plain rectangular chip design, c) Flow patterns in HB design and d) Flow patter in the plain chip design.

For biological applications, especially on research of target (cells)-receptor (biomolecules) binding, the laminar flow conditions in microfluidics can be problematic. A particular issue with microfluidic based immunoaffinity capture of CTCs is that sample flows being laminar means that flows including the targets and biomolecules do not mix and flow in parallel. This means that the target and bioreceptors on device surface may not have sufficient chances to initiate binding. To tackle this, Stott et al.[49] (2010) were one of the first who utilised the Herringbone chip technology (Fig. 5) developed by the Whitesides group[50] in 2002 that induced chaotic mixing in micro flows inside the devices. This ensured that the cells or target molecules flown through the device have ample and interacting environment to hit and bind against the bioreceptor functionalized surfaces and structures. Our research outputs presented in this thesis also exploits the advantages of this design for maximal capture of tumor cells. The concept of inducing chaotic flow inside a microfluidic channel is presented by the schematic below.

1.5 Global applications of microfluidics and uses in CTCs enrichment

Current microfluidic systems have been developed exploiting the unusual flow properties of the organosilicon polymer polydemethoxysilane (PDMS, discussed in more detail in Chapter 3) in the

past two decades for a diverse range of applications including materials science, cellular biology, chemical synthesis, biosensors point-of-care (POC) diagnostics, and cell sorting techniques. Whitesides et al. pioneered the fabrication technology of microfluidic devices in PDMS[51]. This group started flow mixing, patterning of biomaterials, synthesis of metals inside channels to name a few applications of microfluidics on PDMS based simple Y shaped channels. Soon, the need for multiple processing and integration of multiple components arose and Quake et al. produced the first microfluidic large-scale integration device of active mixing and valving components[52]. The so-called microfluidic comparator chip including 2056 microvalves and 256 chambers for complex fluid manipulation was the first multiple layered multi component fluid flow and valving technique.

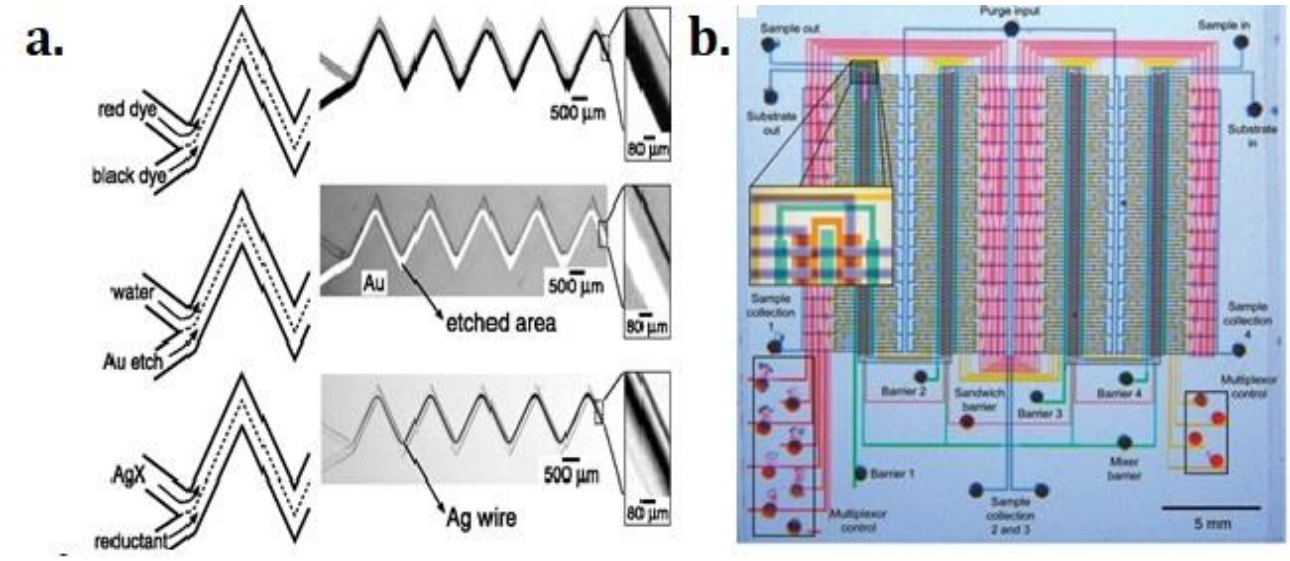

Figure 6. a) A zigzag microchannel design from the Whitesides group for material patterning on surfaces. b) The Microcomparator chip from the Quake group for multimixing fluids

While most of the earlier publications in microfluidics appeared in engineering journals, the unparalleled advantages of microfluidic technologies over traditional macro scale methods in biomedical research is proven[53]. Microfluidics can act as an efficient and versatile tool for fluid processing and cell enrichment, isolation and sorting. The use of microfluidics in cancer related research has also escalated since early 21st century with 20 times more publications now since 2001 sourced through google scholar. This number compared with the overall microfluidics publications show that roughly over 38% of publications relating to microfluidic based research are focused on cancer related topics. Figure 7 shows this comparison in a chart view of number of publications in microfluidics and publications in microfluidic based research in cancer studies.

Enrichment of the CTCs with microfluidic methods has been highly sought and the unique ability of microfluidics to manipulate cells and other biological specimen in biomimetic microenvironments has been reported widely [29,46,54-56]. Microfluidics offers the tools to create micro-environments that have close resemblance to those biological environments *in vivo*. Recent cell recognition modules

using microfluidics have been through fluorescent label and image processing based [34], magnetic bead based[30] and label free based technologies [29]. PDMS based microfluidic devices are easy to use but take a long time to fabricate involving multiple steps until the final device can be fabricated. A user has to create the initial design, use soft lithography techniques and bond the PDMS chips onto desired substrates that can easily take up to 2 days from the start to the end. A faster technique with rapid prototyping of devices for microfluidics applications is needed. Devices with nanomaterials on the surface of the micro-channels are also being used recently to achieve localized trapping and enrichment of CTCs[16]. The integration of microfluidics and nanotechnology has shown promise for this with its unrivalled manipulation, specificity, preciseness, high throughput and yield in microenvironments.

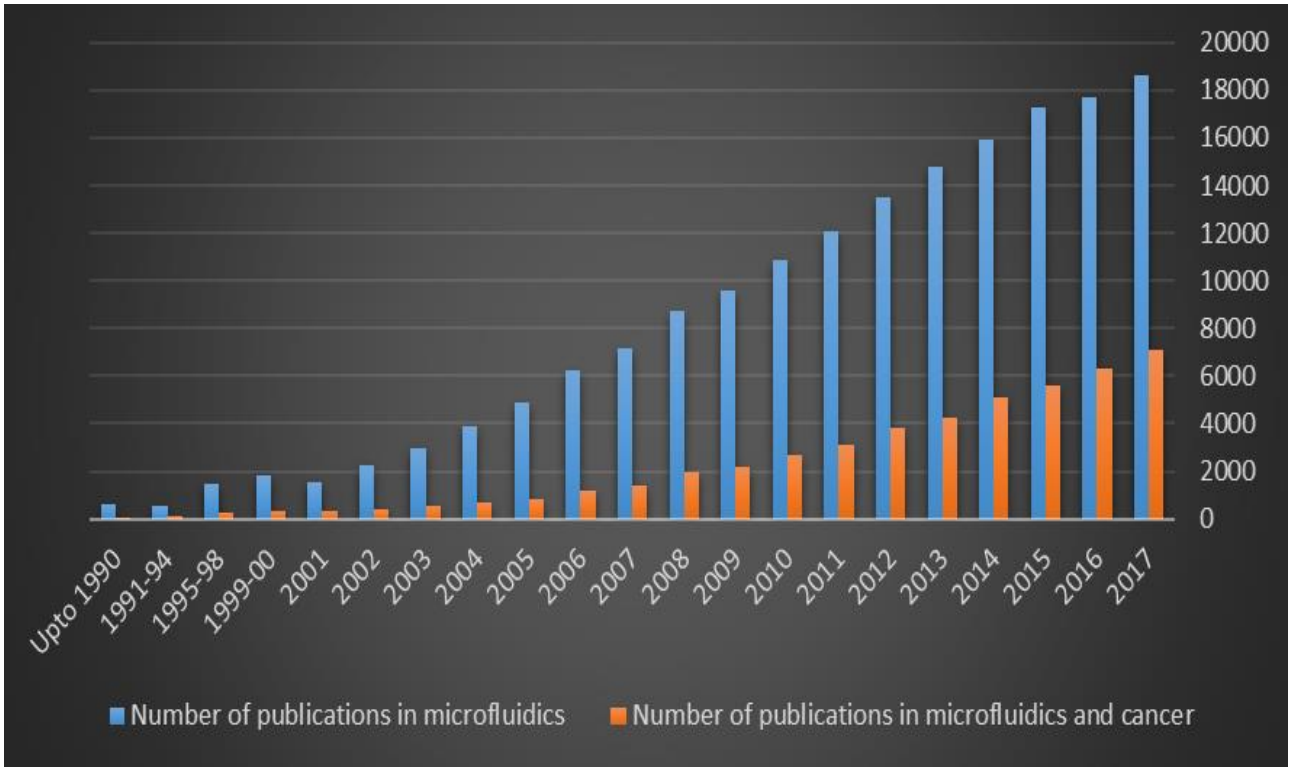

Figure 7. Number of publications with the words 'Microfluidics' and 'Microfluidics and Cancer' sourced through google scholar. As of 2017, over 38% of current microfluidics research is affiliated with research topics of cancer.

1.6 Nanomaterials and functionalized surfaces in microfluidics for cell isolation

Currently, nanotechnology is applied widely in biomedicine and more specifically on CTC isolation and detection for early cancer diagnosis[57]. Nanomaterials have been synthesized on microfluidic devices and also been explored for further applications through these devices[58,59]. Of particular interest for biological applications on microfluidic devices are the nanomaterials for the surface

functionalization of the substrates. These nanomaterials can create nanostructured surfaces that can be very useful for a wide range of applications in biology and medicine. Nanostructured surfaces are known to enhance surface roughness and interactions between substrate and target cells as compared to flat substrates thus increasing cell capture affinity. These nanostructured surfaces inside micro channels also mimic the cellular environment thus enabling realistic capture and detection. This section focuses on how both synthesised nanomaterials and patterned nanostructures on microfluidic devices have been used as nanostructured surfaces for CTC isolation and detection.

CellSearch™, the most widely used CTC isolation platform, uses magnetic nanoparticles functionalized with antibodies against EpCAM, a glycoprotein expressing oncogenic potential and commonly used as a diagnostic marker. This technology is not useful to achieve isolation of CTCs from a heterogeneous CTC sample expressing multiple genes and negative EpCAM profiles. Most of the nanostructured surfaces employed for CTC isolation also use coating of capture agents like anti-EpCAM which is an antibody for capturing EpCAM[60].

Demonstrating one of the first nanostructured surfaces system, Park et al. devised gold nanocluster (Au-NC) coated silicon nanowires to capture cancer cells as well as to irradiate them with a near infra-red light[61]. Wang et al. used the Herringbone (HB) chip and introduced nanostructured silicon substrate to enhance interactions between cells and antibody binded materials and achieved capture efficiency of 95% in artificial samples[62]. The NanoVelcro chip developed by Tseng et al. used silicon nanopillars to isolate MCF-7 breast cancer cell lines with a 45-65% capture efficiency[28]. The NanoVelcro chip was further optimized using polymer nanosubstrates for single CTC isolation[63,64]. Wen et al. used magnetic nanospheres for CTCs capture and detection with a capture efficiency of more than 94% in whole blood[65]. Stimuli responsive polymers have also been used to capture and release cancer cells reversibly on chip by controlling hydrophobicity[66]. Earhart et al. used magnetic nanoparticles for high throughput capture and release of labelled cells in their magnetic sifter chip[67]. Nagrath et al. developed a chip with high sensitivity in capturing CTCs by functionalized graphene oxide nanosheets[13] with a capture efficiency of ~73%. This so-called GO chip uses graphene oxide functionalized gold patterns to perform selective binding of antibodies to target cancer cells. The efficiency of this chip is reportedly lower compared to other techniques, but this device indeed opens up a new nanomaterial based capture of CTCs.

It is also the motivating science for this thesis. Hammond et al. devised a herringbone embedded microfluidic chip, which used gold nanoparticle binding to achieve enhanced isolation and release of CTCs[68]. Chandra Ray et al. have produced a hybrid graphene oxide surface based chip for label-free detection of malignant melanoma from blood[69]. This same group also developed an iron magnetic core-plasmonic shell nanoparticle for targeted isolation of CTCs[70]. Bardhan et al. used graphene oxide nanosheets binded with bound antibodies to achieve high efficiency of capture of cancer cells from

whole blood[71,72]. Employing microfluidics can be a highly powerful tool in capturing CTCs as well as for their detection in further prognosis studies. However, most of the research in this field fails to address some critical issues in CTCs capture including non-specific binding of cells and heterogeneous species capture and detection in the same device.

1.7 Graphene and graphene oxide- introduction and use in CTCs isolation

Graphene is a two-dimensional (2D) material where flat monolayers of carbon atoms are tightly packed in a 2D honeycomb lattice. It is the main building block for carbon materials with all other dimensionalities and has some interesting physical properties reported. In 2004, Geim and Novoselov isolated graphene experimentally from bulk graphites for the first time. Initial research in graphene was limited to theoretical understanding[73-75] and applications in nano-electronics, nanocomposite materials, optics and semiconductors[76-79]. Synthesis of graphene has been explored through a variety of different techniques[77,80-84]. Graphene has been explored for its applications including biological systems in developing biosensors[82,85,86] and drug delivery devices[87-91]. As graphene is very thin, its coatings do not affect the wetting behaviour for surfaces[92], i.e. a graphene coated surface has almost similar contact with an aqueous specimen as an uncoated surface. This is very important for applications in bio-sensing where contact with aqueous systems is a prerequisite.

Graphene oxide is a single layer form of graphite formed by treating graphite with strong oxidizers and then dispersing in basic solutions like water. While the application of graphene oxide has been seen in diverse research areas [78,79,85,90,93,94], our project focused on its value on the isolation and detection of circulating tumor cells. A Harvard group led by Sunitha Nagrath were the first to isolate CTCs from blood samples using functionalized graphene oxide nanosheets on a patterned gold surface[13]. This same group have also developed a system with tunable thermally responsive polymer-graphene oxide composite for reversible capture and release of CTCs[95]. These two devices present novel CTC trapping technology but do not offer an on chip multiple CTC detection platform. Most of the other reports on using graphene oxide to capture CTCs have been on platforms developed not using microfluidic systems. Li et al. have reported a platform with an antibody modified reduced graphene oxide films to capture CTCs[96]. Nellore et al. have demonstrated an aptamer-conjugated graphene oxide membrane for efficient capture and detection of multiple CTCs[97]. More recently, Bardhan et al. reported enhanced cell capture on graphene nanosheets using oxygen-clustering[71]. Relatively little attention has been paid to using graphene oxide as a potential material for enumeration and enhancing the isolation of CTCs except for a few handful of published articles. Table 1. presents the list of CTC isolation technologies developed using microfluidics, their samples used, flow rates and capture efficiencies.

Table 1. Summary table of various CTC isolation technologies developed using microfluidics

Device name	Capture efficiency (%)	Clinical test samples	Flow rate (mL hr^{-1})	Capture technique	Purity (%)	Ref.
CTC-chip	>60 65	- NCI-H1650 in whole blood - NCI-H1650, SKBr-3, PC3-9, T-24 in PBS	1	EpCAM- affinity	50	[22]
HB-chip	92	PC3 cells (prostate) in blood	1.2	EpCAM- affinity	14	[49]
GO chip	>85	MCF-7 cells (breast) in blood	1	EpCAM- affinity	-	[13]
GEDI Chip	85	LNCap cells in blood	1	EpCAM- affinity	68	[98]
NanoVelcro Chip	>80	LNCaP, PC-3, C4-2 (prostate) in blood	0.5	EpCAM- affinity	-	[63]
HTMSU	97	MCF-7: citrated whole rabbit blood	2	EpCAM- affinity	-	[99]
Magnetic Array	80±20	MCF-7: Endothelial cells:	-	EpCAM- affinity	-	[100]
Magnetic micropillar	>70	DMEM: HCT116	0.05	EpCAM- affinity	-	[101]
Aptamer microchip	>80	RPMI medium: CCRF-CEM, NB-4	0.72	DNA-aptamer	~97	[102]
SB Microfilter	83±3 78±4	MCF-7 MDA-MB 231	-	Size based (filter pores)	-	[103]
Aptamer Nanosubstrates	>80	In artificial blood A549	1	DNA-aptamer	~99	[104]
Dean Flow	>80	MDA-MB-231, MCF-7 and T-24	56.25	Size based (hydrodynamic)	-	[105]
p-MOFF	93.75 91.60	MCF-7 MDA-MB-231	36	Size based (hydrodynamic)	-	[106]
Nanowire substrate	65.1±25.2	In culture medium A549	-	EpCAM- affinity	-	[107]
Nanoroughened glass	89-96 93-95	In PBMCs: MCF-7, MDA-MB-231 In lysed whole blood: MCF-7, MDA-MB-231	-	Label free	-	[108]
Spiral Shape	96.3 81.2	MCF-7 and MDA-MB-231 from breast carcinoma cells, positive and negative CTCs	9 9	EpCAM-affinity	-	[109]
DEP	>95	MDA-231 normal cells	0.3-6	Label free	-	[110]
NegCTC-ichip	96.7±1.9 97.0±1.7	Whole blood: MCF10A Whole blood: MCF10A-LBX1	8	CD45 and CD15 affinity	-	[111]

1.8 Perspectives and challenges of microfluidic based CTC isolation devices

Circulating tumor cells (CTCs) have great potential to serve as reliable biomarkers via liquid biopsies for minimally-invasive cancer detection and therapeutic monitoring. Their isolation and analysis is highly pursued in translational cancer research. Microfluidics combined with nanomaterials are utilized as a powerful tool in the isolation and detection of CTCs and have shown promising results with high purity, throughput and versatility for capturing CTCs. However, due to the rarity of the CTCs and their heterogeneity, there are still many challenges to overcome to achieve commercially viable, easy to use and cheap microfluidic CTC isolation devices for mass production. Especially for affinity-based methods, not all cells express the same basic oncogenes from the antigens of their protein materials like EpCAM. This hinders capture of heterogeneous CTC samples with both positive and negative CTCs.

Microfluidic devices have certainly improved capture efficiencies with embedded nanomaterials and nanostructures, but these platforms are yet to solve non-specific binding affinities. Also, cell-ligand interactions during fluid flow in nanomaterials based microfluidic devices are not sufficient enough which affects throughput. Devices integrating multiple techniques have removed some of these issues but are yet to achieve high throughput and ease of use due to their complex fabrication protocols. New CTC devices should also possess multiplex detection of heterogeneous samples as well as removal of false detections. Future microfluidic based CTC isolation platforms should be integrated for high purity, versatility, and specificity, throughput and multiplex detection in easy to fabricate and analyse devices. The following chapter presents our approach and the research methods we have developed and optimized during this thesis period to overcome some of these issues for isolation of CTCs in nanomaterial functionalized microfluidic devices.

Chapter 2.

Experimental methods: materials, instrumentation and analytical tools

This chapter describes the experimental methodologies, the tools and techniques and the materials used in the research project which is the subject of this thesis. The project requires functionalization of nanomaterials and biomolecules on different substrates, tools and techniques for the fabrication of microfluidic devices, and finally it uses analytical tools for measurements and results. Additionally, we discuss the reasons for choosing a particular material or a technique where relevant for the successful completion of this research work. The main aim of this research project was to functionalize nanomaterials in microfluidic devices, characterize its binding affinities with biomolecules and use this platform to capture CTCs. We aimed to find out if the nanomaterials we selected provided a platform for capture of CTCs inside microfluidic devices. We predict that nanomaterials we used would increase capture sites and capture efficiencies on functionalized surfaces compared to non-functionalized surfaces.

2.1 Device design and fabrication procedures

As the flows in micro channels under normal operating conditions are laminar, molecular diffusion across the channels is low and it is difficult to promote turbulent flows and mixing. The science inside the device is that of immunoaffinity capture and this requires maximum interaction of the biofluids with the nanomaterials functionalized surface. The chip design follows the concept of chaotic mixing in microfluidic devices developed by the Whitesides group[50]. The concept of chaotic mixing and why it is needed for our devices has already been discussed in chapter 1. A schematic of our own version of the device with the dimensions is shown in figure 9. below with a detailed version in the appendix:

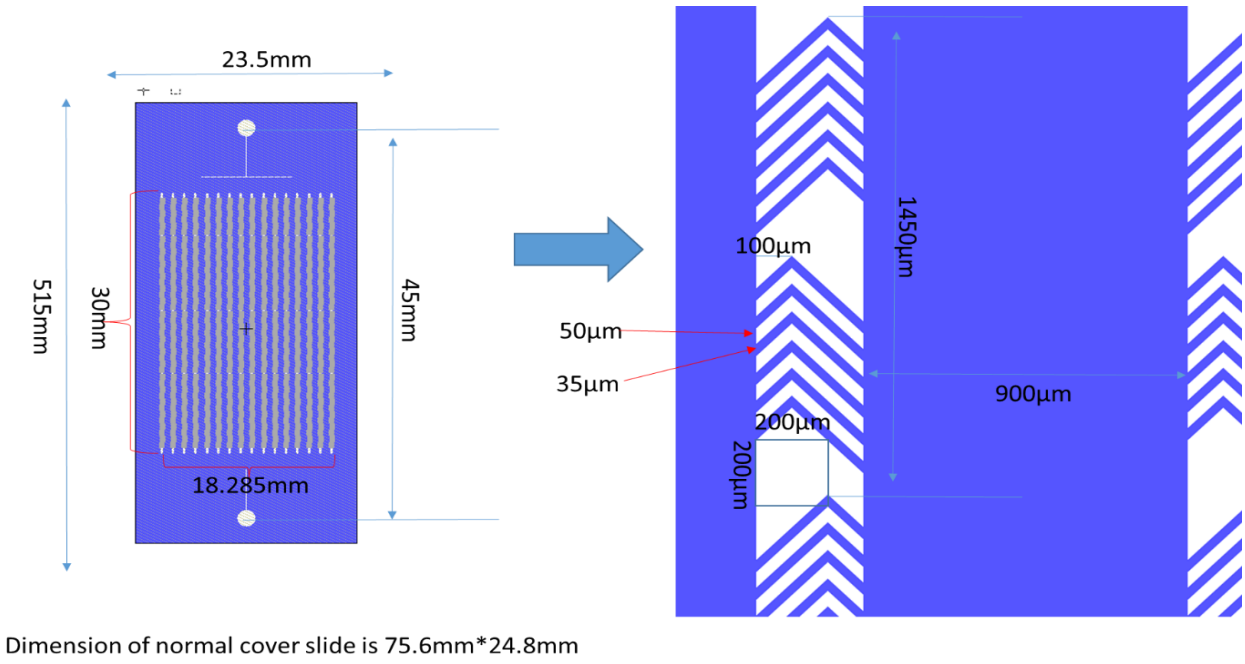

Figure 8. A schematic of the Herringbone (HB) structured microchannels used for the PDMS based microfluidic devices.

The master mold design has a single inlet and outlet for fluid flow. There are 16 microchannels in total in the design. Each microchannel has a height of around 50 microns and the herringbone pit has an additional 30 microns as height. The total length between the inlet and outlet is 9mm. The width of each microchannel is around 300 microns. The author acknowledges Dr. Jiang for fabricating the master mold design which was patterned on a silicon wafer.

Most microfluidic devices today still use photolithography to fabricate SU-8 masters after which the designs of the microchannels can be imprinted to the PDMS stamps via soft lithography. Newer techniques like 3D printing can be used for mask fabrication and these techniques will be employed in ongoing research. Soft lithography is an extension of standard lithography technique that replicates structures using stamps, molds and photomasks. It is a versatile method with much lower costs compared to traditional photolithography.

Photolithography is a photo-imaging method which transfer geometric patterns from a mask design to a substrate (wafer). Briefly, a silicon wafer was spin-coated with the appropriate photoresist depending on the height desired. In this case, SU8 was used as the photoresist. It is a negative photoresist that can be polymerized with UV exposure and the sections that are unexposed are removed. Printing of the micro channels in the master mold requires a special process that is described in the schematic (Fig. 11.a). Depending on the number of channel layers required for the device, the process has to be repeated for multi-layer structures in the devices. For the fabrication of the PDMS stamps, a mold replication technique (Fig. 11.b) is necessary.

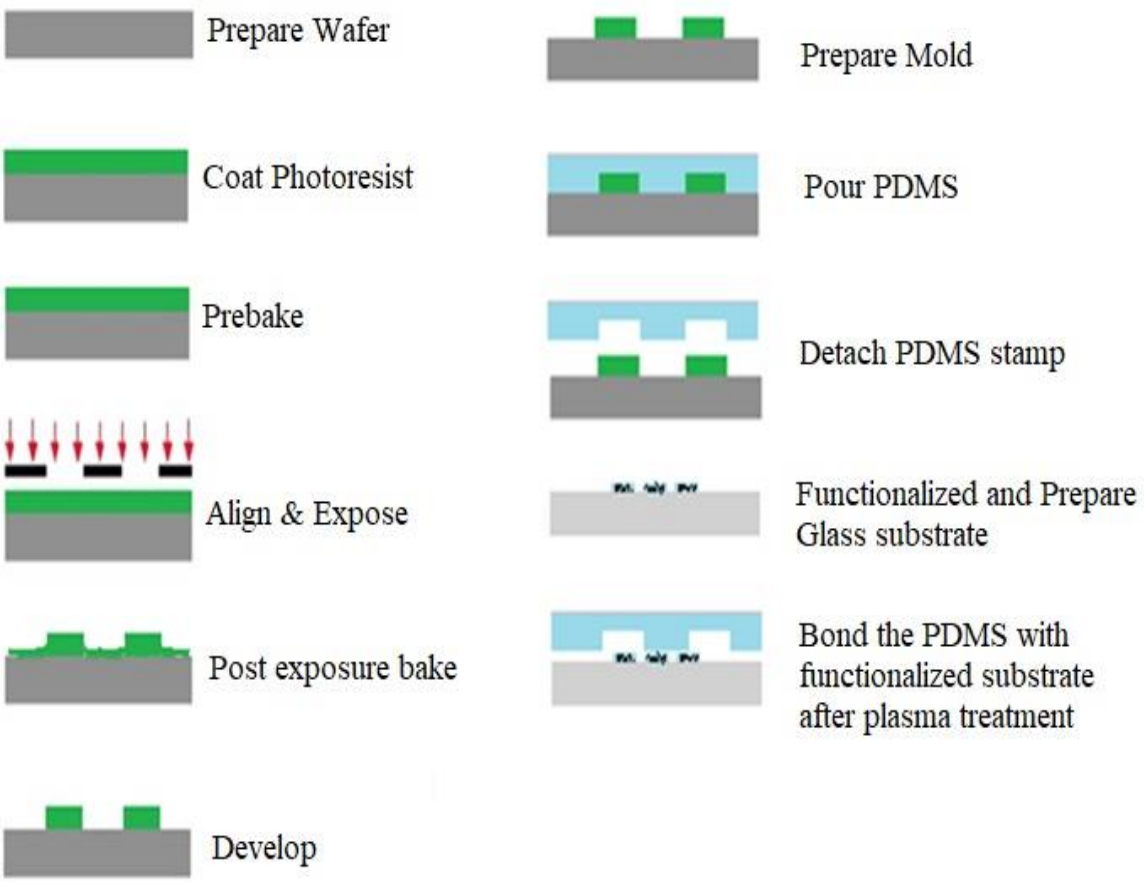

Figure 9. a) Schematic for the master mold fabrication on a silicon wafer and b) Technique for microchannel design replication based on molding with PDMS with further functionalization steps

This approach was used to imprint the microchannels on a polymer called Polydimethylsiloxane (PDMS), a polymer that belongs to the group of polymeric organosilicon compounds referred to as silicones. It is one of the most widely used compounds for a variety of applications in science and industry. Most of the techniques fabricating microfluidic devices use PDMS as the material for the soft lithography-based fabrication of microchannels. PDMS has atypical rheological properties that are well documented and has been explored for various applications in industry and science.

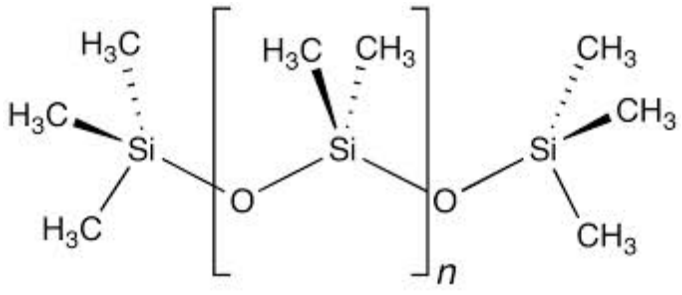

Figure 10. Chemical Structure of Polydimethylsiloxane (PDMS).

The special rheological properties of PDMS for fluid flow makes it a good material for microfluidic science. All the devices fabricated for this project used PDMS based stamps as the channel layers for the experiments.

Content of pages 21 and 22 removed from full access at the request of the author (Copyright holder). 2.9.2019

2.2.5 Antibodies

Antibodies, also called immunoglobulins, are Y-shaped blood proteins that are naturally produced by the body's immune system to prevent pathogens and cancerous cells from doing damage to the body. Antibodies recognize specific antigens (toxins) produced by invaders like bacteria, viruses or more relevant to the project: by cancerous cells. The antibody protein shape (Fig. 14) is by nature designed in a way similar to that of locking system such that each tip of the 'Y' shape has a 'paratope' (a lock) that specifically binds to one particular 'epitope' (a key) of an antigen. This binding force is strong and once tagged the cell is either inhibited or isolated. Millions of antibodies possess different tip structures at a small region known as the hypervariable region that allow millions of different binding sites and structures.

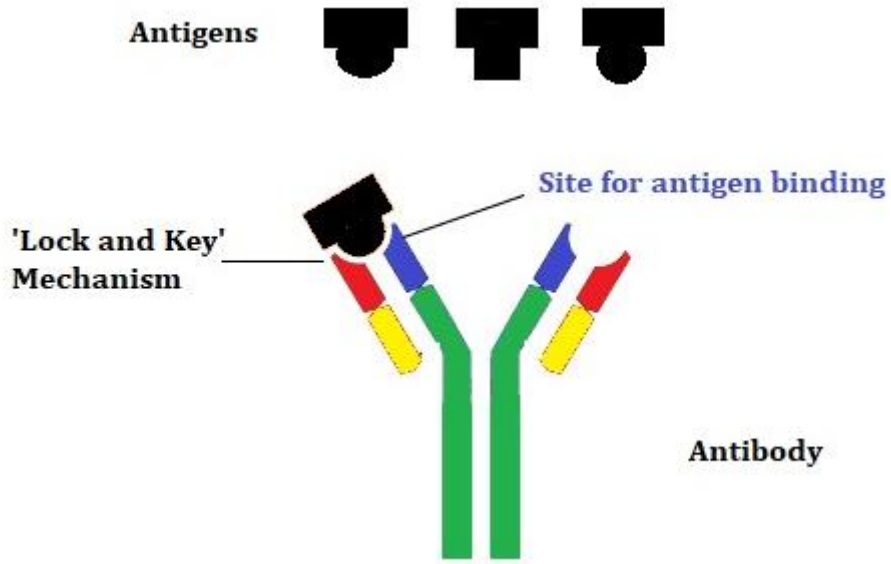

Figure 13. The 'Lock and Key' binding mechanism of Antibody- Antigens

For the present project, we used three different antibodies as bio-receptors to capture our cell target antigens and to test binding affinities on graphene oxide functionalized and non-functionalized surfaces:

i. Anti-Human IgM Primary antibody [EPR5539-65-4] (Alexa Fluor® 488)
   -Used for binding affinity tests on PDMS and GO functionalized glass surfaces)

ii. MIL-38 (An IgG1 murine monoclonal antibody targeting Glypican-1 (GPC-1) antigen
   -From the company Minomic® for DU145 and C3 cell binding tests)

iii. Anti-EpCAM (Antibody targeting Epithelial cell adhesion molecule (EpCAM) antigens)
   -Used for general tests and negative tests

Dr. Nima Sayyadi of the Department of Molecular Sciences at Macquarie University and CNBP kindly provided all the antibodies used for this project.

2.2.6 Cell lines

Two different cell lines were used to i) compare the capture efficiency (%) in a PEGylated GO functionalized glass surface based device vs a non-functionalized chip and ii) Compare the specificity of the antibody towards DU145 and the negative cell line C3. Both of our cell lines were kindly provided by Victoria Yan Wang from Macquarie University and CNBP.

i. DU145

   This is a classical human prostate cancer cell line along with PC3 and LNCaP. They do not express prostate specific antigen (PSA) and have been investigated for Glypican-1 expression[38,112]. They are also known to have highly reduced EpCAM expression[113,114].

ii. C3

   A cell line present in blood that expresses the C3 protein[38]. This was used as a negative control to evaluate the specificity of the Mil-38 antibody specificity towards DU145 cells inside the microfluidic device.

2.3 Functionalization of glass substrates and microfluidic biomolecule binding

Graphene oxide functionalization in glass substrates was essential for bio-receptors binding on our microfluidic devices. We studied different techniques for coating graphene oxide monolayer sheets in water and modified some techniques used for this project. More details on the analytical results of varying functionalization parameters and techniques are presented in the results chapter. We discuss here the two essential components of functionalization inside our microfluidic devices:

a. Nanomaterial functionalization

   The nanomaterial functionalization on glass substrates in this project follows a method developed by Nagrath et al. with some modifications and coating technique variations. Graphene oxide monolayer sheets in water were non-covalently functionalized by amine functionalized PEG phospholipids before spin coating on glass substrates. The hydrophobic lipid chains of the lipids material are strongly immobilized on the graphene oxide functionalized glass surface. Oxygen plasma treatment of glass substrates before spin coating was required for a uniform coating. After spin coating, the glass substrates were kept on a sealed petridish in the cleanroom facility for 24 hours and washed with (DI) water. The plasma treatment variation and characterization images through SEM and AFM are presented in the results chapter. Here we show bright field images of plasma treated and untreated glass surfaces:

Figure 14. Images of Glass slides with and without oxygen plasma treatment before GO coating

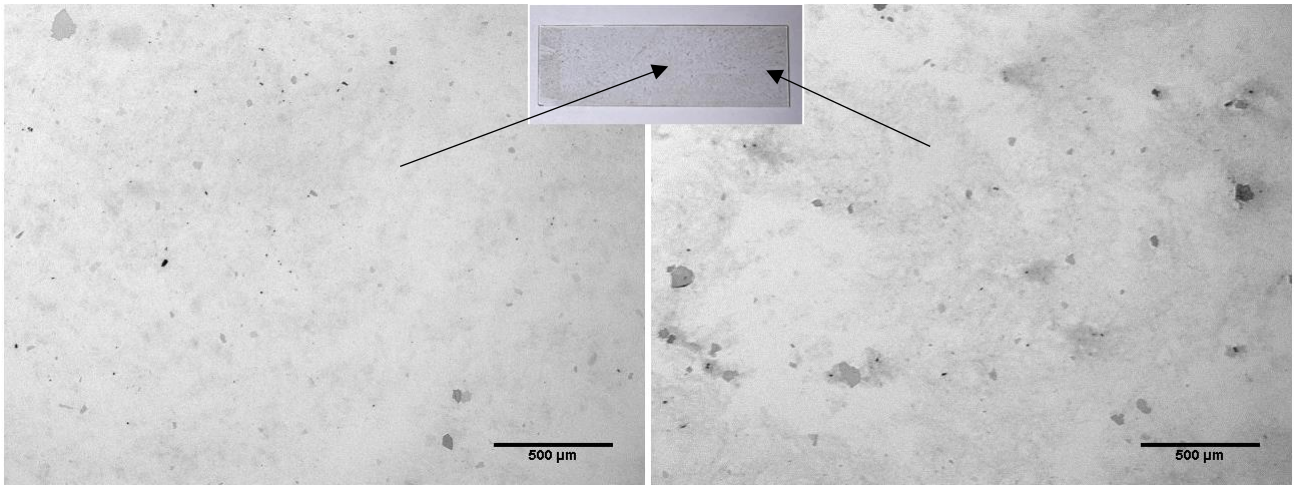

Figure 15. Bright field images of GO functionalized glass slide (Fig 14b)

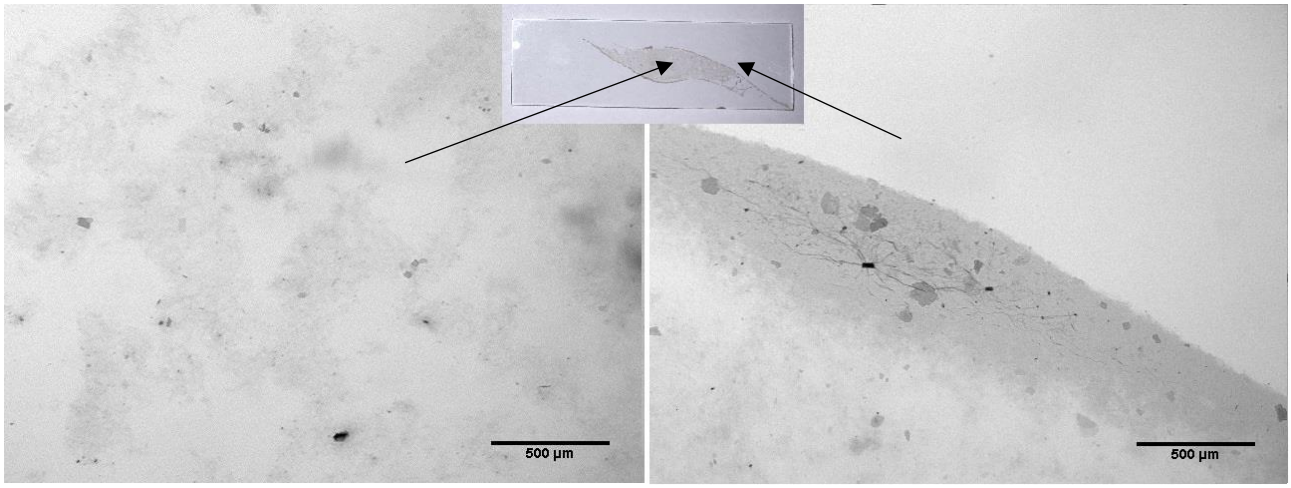

Figure 16. Bright Field images of GO functionalized glass slide (Fig 14c)

b. Biochemical functionalization and flow through microfluidic devices

GMBS (N-γ-maleimidobutyryl-oxysuccinimide ester) is a cross linker that is reactive towards amino and sulfhydryl groups. It was flowed through the microfluidic device at rates described in the results section. This cross-linker has NHS esters (N-hydroxysuccinimide esters) that react with the amine groups of the PEGylated graphene oxide structures to form amide bonds. It also links with the sulfhydryl groups of the proteins. After GMBS, Streptavidin and antibodies (Biotinylated EpCAM, Mil-38 and Ani-Human IgM) were subsequently flown for interactions inside the chip depending on the experiments performed. More details of all the functionalization procedures are in the appendix section. A schematic (Fig. 18) shows the entire capture mechanism in the device.

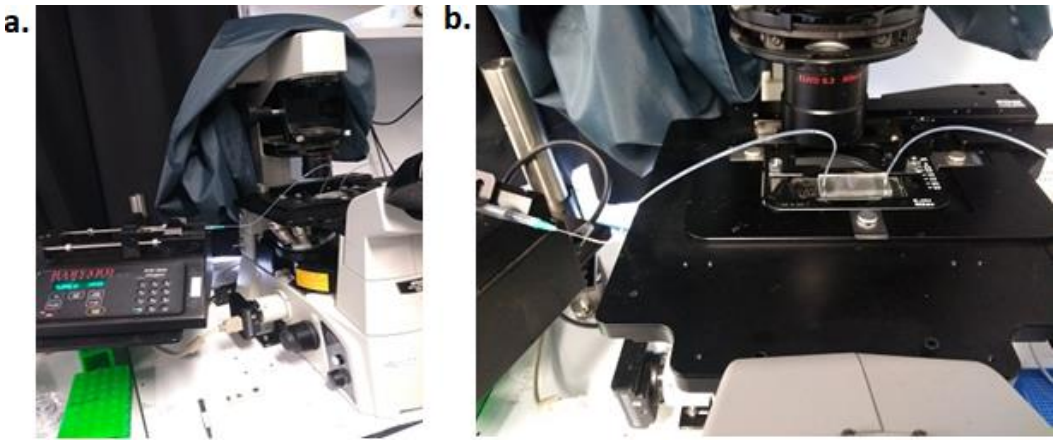

Figure 17. a) The Microfluidic fluid flow system with the syringe pump and the microscope. b) The microfluidic device on the stage with inlet tubing from the infusing syringe and outlet tubing.

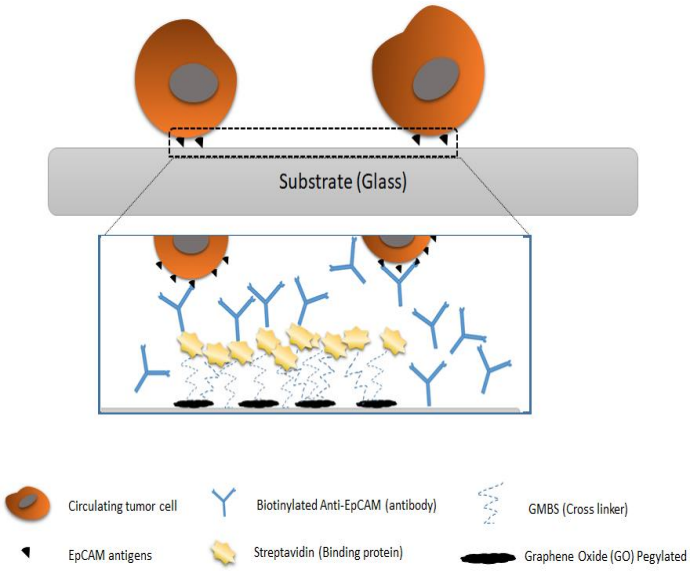

Figure 18. A schematic illustration of CTCs capture on Graphene oxide functionalized substrates

2.4 Analytical tools and Instrumentation

i. Scanning Electron Microscopy (SEM)

SEM is an electron microscope where a focused electron beam scans over a surface to create topographical images of the specimen. The scan takes place in a raster scan pattern. SEM was used in this project to verify and produce images of the Graphene oxide coated glass substrates, to show their characteristic depths and to compare the results at different spincoating speeds to find out the best rpm for spin-coating the nanomaterial in a uniform way. SEM was available at the microscopy facility of Macquarie University. Equipment used was the JEOL JSM 7100F FESEM – Field Emission Scanning Electron Microscope. SEM images were obtained with the help of Chao Shen at the Microscopy Unit.

ii. Atomic force microscopy (AFM)

AFM is a type of a scanning probe microscopy with a very high resolution. It overcomes the drawback of STM/SEM of requiring conducting surfaces and can perform imaging for any surface such as glass, polymers or biological samples. AFM was used in this project to measure the height of the graphene oxide structures coated on glass. SEM and AFM was done consecutively to image and characterise the structures on the glass slides. AFM was available at the microscopy facility of Macquarie University. Equipment used was the Bruker Innova AFM - Atomic Force Microscope. AFM images were obtained with the help of Chao Shen at the Microscopy Unit.

iii. ImageJ/Fiji

Image J is an image processing program that was inspired by NIH Image for Macintosh. Written on Java and Python, it can calculate area and pixel value data of user-defined selections. Fiji is a version of a plugin loaded ImageJ which was used for image processing and data analysis in this project. Profile plots of fluorescent materials and antibodies as well as 3d images based on fluorescence intensity were made through this software. Spatial measurements were also made through this software in all of the images unless otherwise noted.

Chapter 3.

Results and Discussions

This chapter presents the measurements and characterization of the nanomaterial graphene oxide (GO) functionalized onto glass surfaces. Morphologic characterization, spin-coating techniques, height measurement of the nanostructures are presented and discussed. The added benefits of using nanomaterial rich surfaces in cell capture efficiency are also discussed. Finally, the chapter ends with the results of binding affinity variation measurements of antibodies on graphene oxide functionalized glass surface vs non-graphene oxide surfaces.

3.1 Graphene oxide functionalization on glass and profiling with SEM and AFM

Glass substrates were functionalized with graphene oxide using a technique based on spin coating the surface[115]. Functionalization procedures for this research have already been discussed on experimental methods in Chapter 2. After functionalization, SEM and AFM measurements were taken to verify the patterning of the Graphene Oxide layer coat and to measure the height of the GO nanostructures obtained on the spin coated glass substrates. We observed that oxygen plasma treatment on glass surfaces helped coat a uniform layer of graphene oxide whereas spin coated surfaces without pre plasma treatment showed coating only on the central area and not on the sides (Fig. 19 and 20). The reason for this is that oxygen plasma exposure towards glass surface activates

the surface energy of the glass decreasing contact angle for liquids making it more hydrophilic which promotes uniform coating. Fig 19 shows SEM image of graphene oxide structures (layers and curl like features) on glass, whereas it is absent on the sides of the glass surface (Fig 20). This non uniform coating is due to the absence of oxygen plasma treatment as discussed earlier.

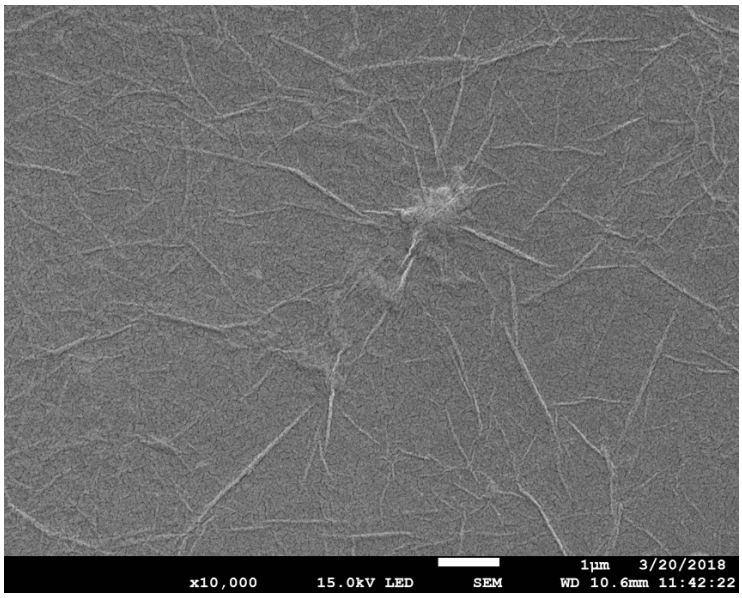

Figure 19. SEM image of GO coated glass surface at the centre without oxygen plasma treatment

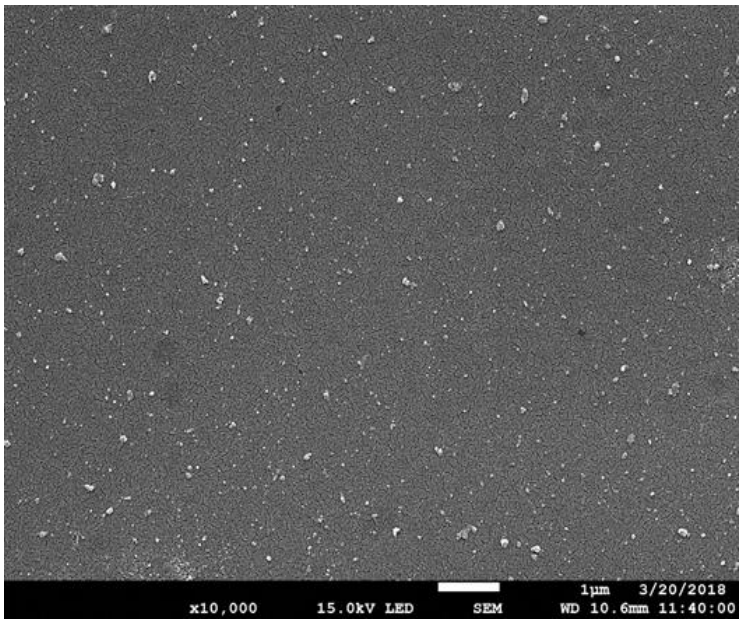

Figure 20. SEM image of GO coated glass surface at the sides without oxygen plasma treatment.

Different spin coating rates were tested for the spin coating of the GO nanomaterial, and the optimal rate of 2500rpm was determined after both experimental observation and previously described studies of uniformity rates for a 2mg/mL concentration GO solution in water. SEM images (Fig. 21 and 22) represent the oxygen plasma treated glass slides with graphene oxide functionalization.

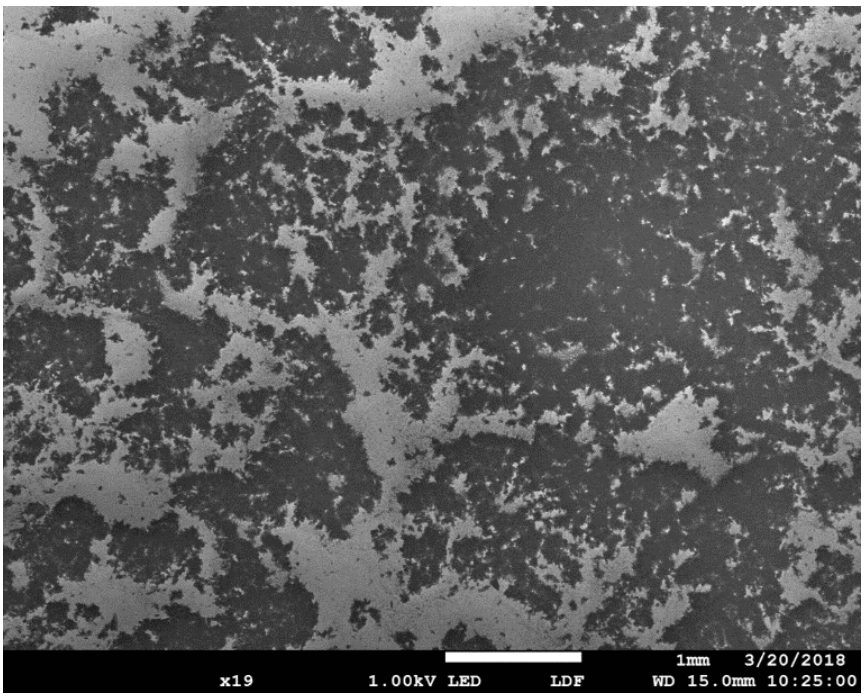

Figure 21. SEM image (19X) of Graphene oxide coated glass surface.

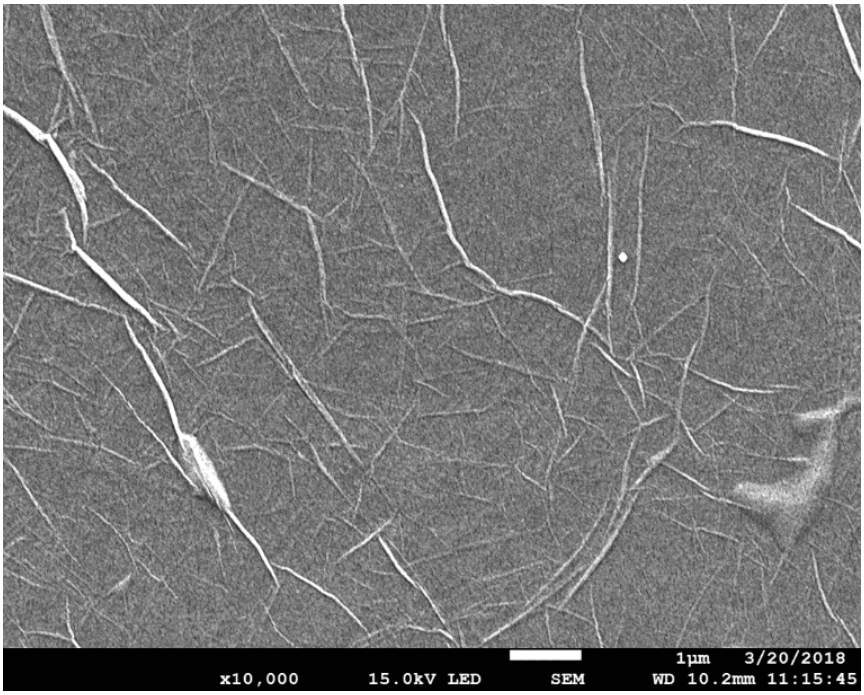

Figure 22. SEM image (10,000X) of Graphene oxide coated glass surface with oxygen plasma treatment.

The SEM images above show the coating of GO structures on an oxygen plasma treated surface. As revealed from images above compared to untreated glass surfaces, oxygen plasma treated glass could be functionalized with graphene oxide more uniformly and can easily meet the cellular scale dimensional requirements (~10 microns) for capture. Immediately following SEM, these glass substrates were examined under Atomic Force Microscope (AFM) for topography and relative average height measurements of the graphene oxide nanosheets and nanoclusters.

Atomic Force Microscopy (AFM) measurements of the GO spin coated substrate revealed the relative average height of GO nanostructures with the aggregated sheets peak height at ~83nm. AFM measurements were taken over a sample area of 5*5 microns. AFM images were taken to verify that GO coated structures were uniform and covering at least the necessary surface dimensions required for biomolecules and cellular scale interactions in microns. The topography images below revealed GO nanosheets as well as colloids with variable heights.

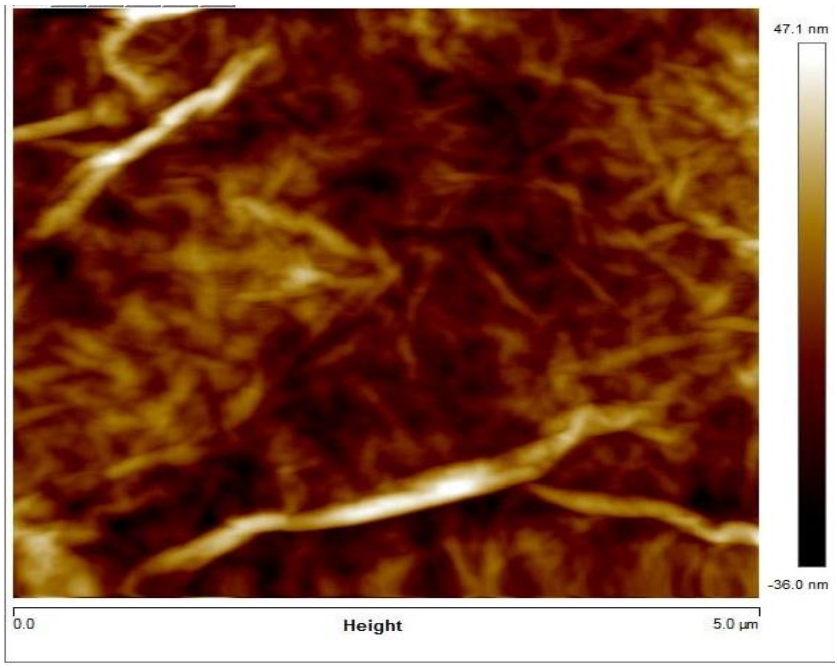

*Figure 23. AFM topographic image of a spot on GO coated glass substrate of a 5*5 micron spot.*

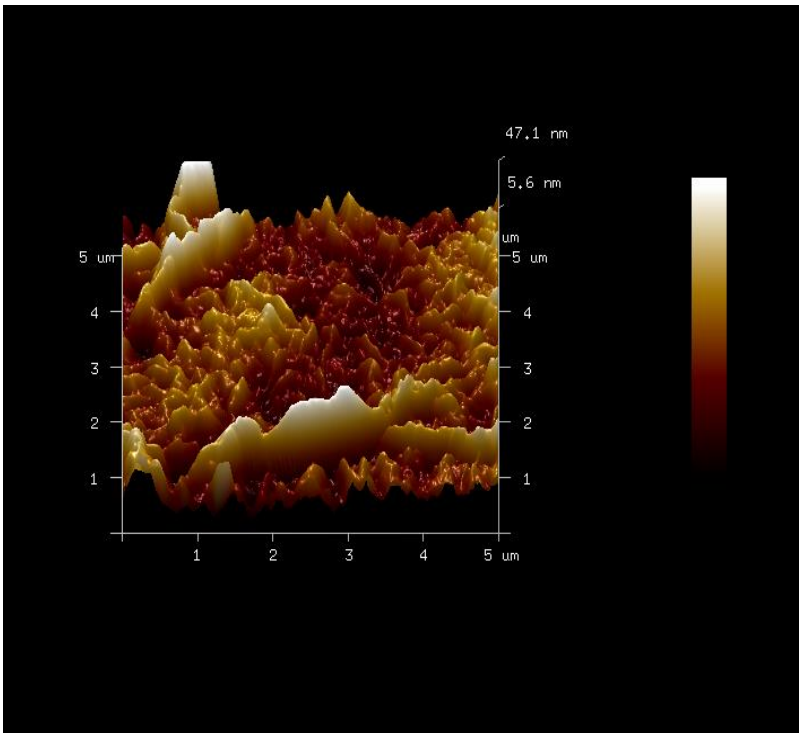

Figure 24. 3d image of Fig. 24's topographic spot. 3d version is only accessible through the NanoScope® Analysis 1.5 Software.

3.2 Fluorescent antibodies binding affinity on different surfaces

For maximal and efficient capture of tumor cells or targets, a microfluidic device needs to be functionalized with bio-receptors with high binding affinity. This capture rate can be affected by a non-specific binding property of biomolecules known as non-specific adsorption (NSA). NSA of biomolecules is a major challenge in microfluidic biosensors. In microfluidic devices, immobilized bioreceptors like antibodies, enzymes and proteins are conjugated with linker molecules that form self-assembled monolayers (SAMs) on the surface of the substrate (glass, silicon, gold, etc). These self-assembled monolayers are prone to non-specific adsorption raising both false positive and false negative results. The three major NSAs that may occur in a bioreceptor-linker molecule system using SAMs have been described previously by Choi et al: a) Where bioreceptors are non-immobilized, b) Where monolayers are formed imperfectly and c) Where the surface SAM on the substrate has defects. These issues can be minimized using some techniques including use of blocker solutions. We used 1% BSA solution in each of our DPBS based solutions of antibodies and cells. The cross-linking agent GMBS is an amine-to sulfhydryl crosslinker that has NHS ester and maleimide reactive groups with shortest arm length (7.3 angstroms) and responds well to the bio-receptors negating the NSA effects due to monolayer formation defects.

To be certain that our system's binding affinity of bioreceptors was higher for the GO functionalized system, we used fluorescent antibodies on a non-GO functionalized PDMS channel surface and GO functionalized glass surfaces. Our aim was to test the binding affinity levels of the antibodies and proteins towards the GO vs non-GO surfaces and do a comparative analysis of the binding in both systems. Both surfaces were functionalized with antibodies at the same time to have similar fluorescence intensity levels. The two different surfaces and their functionalization techniques with their results are as follows:

a. Antibodies binding on dropcasted GO functionalized surface

   Microscopic glass slides were sonicated for 10 minutes. The slides were thoroughly cleaned with iso-propanol and dried with compressed air. PEGylated GO was drop casted on glass slides. The slides were kept under the hood for 2 hours for the PEGylated GO bonding to occur on the glass slides. The slides were then washed with DI water to remove unbounded structures. GMBS, a cross linker was introduced to the slides and allowed to cross link with the PEG molecules and kept under the hood for 30 minutes. The slides were washed again with DI water. Streptavidin, the binding protein which binds the cross linker with the antibodies was introduced in the slides. Then the slides were incubated for 1 hour followed by DI water washing.

Fluorescent antibodies (Anti-Human IgM Primary antibody) were then introduced on the functionalized GO spots on the glass, incubated for 1 hour followed by DI water washing and then observed under the microscope. Fluorescent antibodies were chosen in order to obtain a direct intensity value correlation of the fluorescence signal to the antibodies reported on a GO functionalized spot. *Fiji*, an image and data analysis software package based on Java and Python was used for plot profiles. A rectangular section in an image displays a selected column's average plot values, where the x-axis represents the horizontal distance through the selection and the y-axis represents the vertically averaged pixel intensity. The fluorescence intensity values was recorded and the binding affinity percent after wash with DI water was calculated. Below are the fluorescence microscopy images and intensity curves of GO functionalized spots with fluorescent antibodies:

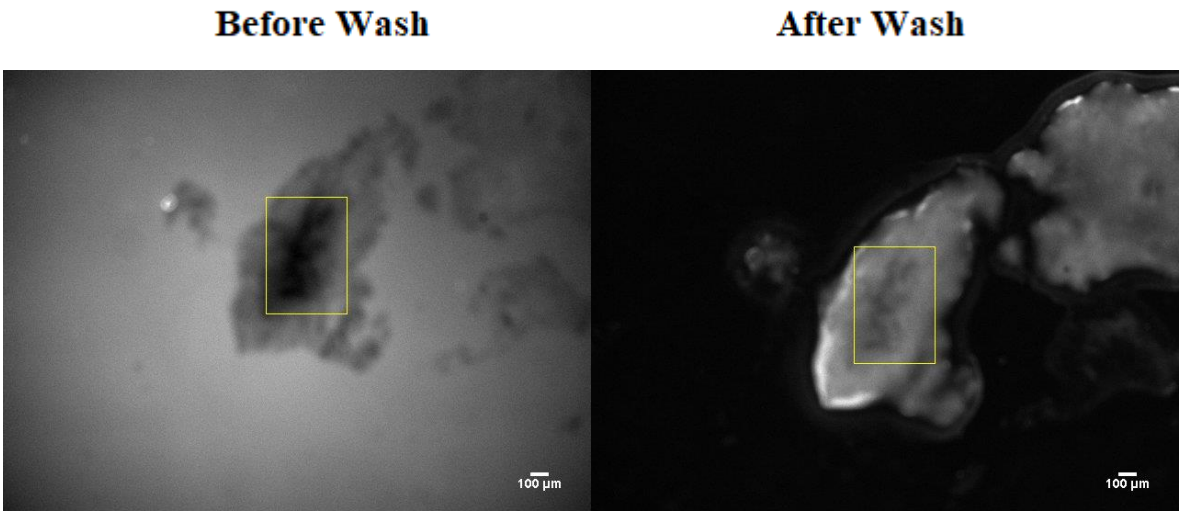

Figure 25. Fluorescence microscopy images of a GO functionalized spot (dropcasted) with antibodies before and after washing with DI water on glass. Yellow selection denotes the area where surface fluorescence intensity values were taken.

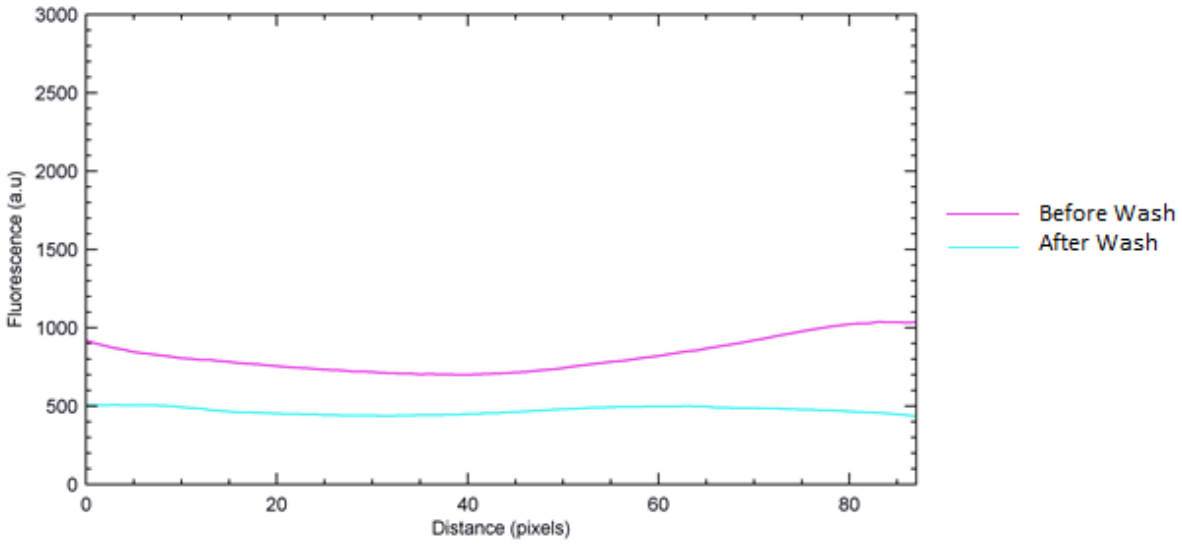

Figure 26. Fluorescence intensity values of antibodies on GO functionalized micro-layers on glass surface before and wash with DI water.

b. Antibodies binding on spin coated GO surface

To have more accurate binding affinity values for our system, spin-coated glass slides with PEGylated graphene oxide were employed. A microscopic glass slide was sonicated for 10 minutes. The slide was thoroughly cleaned with iso-propanol and dried with compressed air. PEGylated graphene oxide was then spincoated on the glass slide. The remainder of the functionalization process was similar to the protocol described for antibodies binding on the drop casted GO functionalized surface. Intensity measurements were performed by Fiji software in the way described previously for GO surfaces.

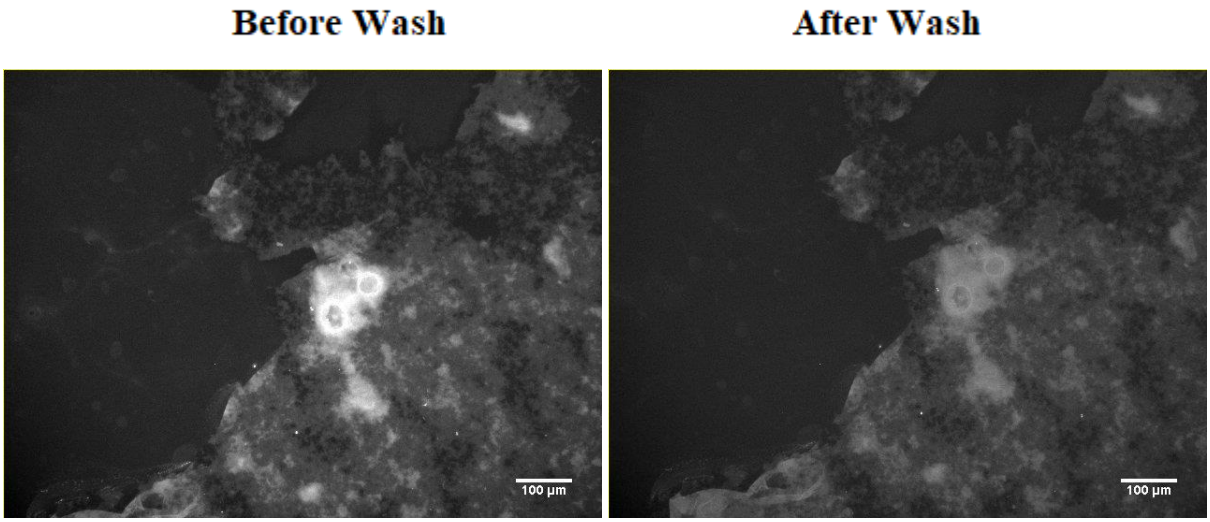

Figure 27. Fluorescence microscopy images of a GO spincoated surface on glass with antibodies before and after washing with DI water. Surface fluorescence intensity values were taken from entire surface.

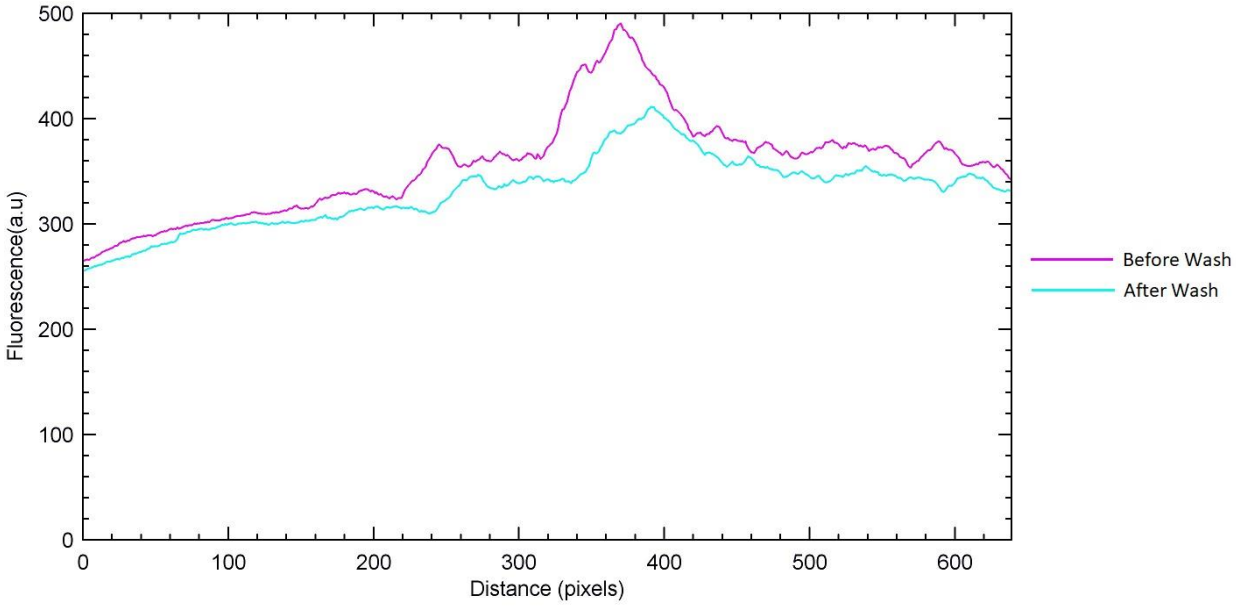

Figure 28. Fluorescence intensity values of antibodies on GO spin coated surface on glass before and wash with DI water.

c. Antibodies binding on plain glass surface without GO

To compare the before and after fluorescence values and influence of GO, plain glass slides without any GO functionalization were prepared. A microscopic glass slide was sonicated for 10 minutes. The slide was thoroughly cleaned with iso-propanol and dried with compressed air. In this case no PEG-GO was present on the glass surface. The exact location for fluorescence values was marked with a black sharpie pen for consistency. The remainder of the functionalization process was similar to the protocol detailed for antibodies binding on the drop casted GO functionalized surface. Intensity measurements were performed by Fiji software in the way described for GO surfaces.

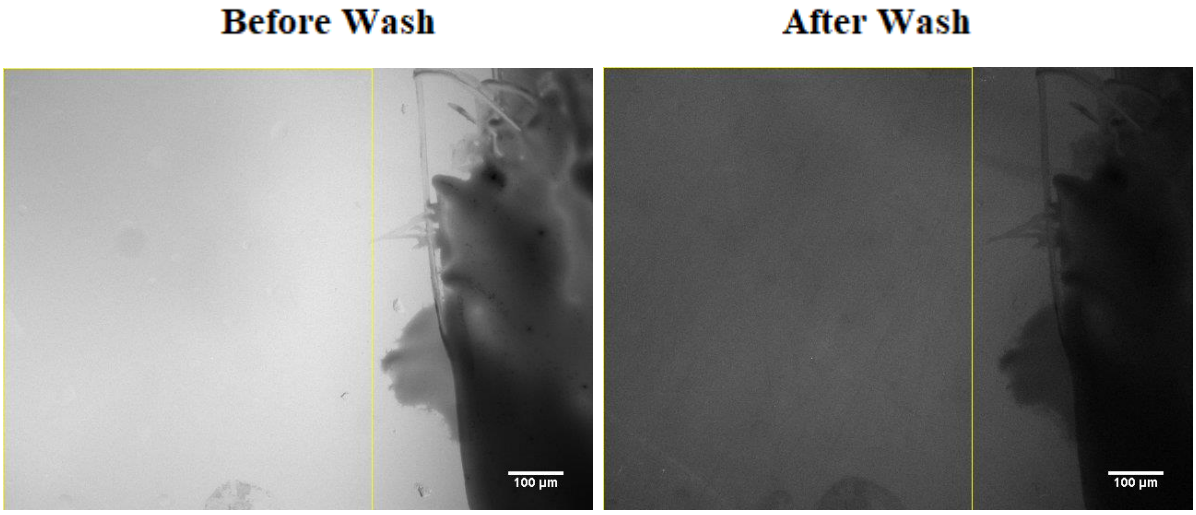

Figure 29. Fluorescence microscopy images of a plain glass surface without any GO functionalization with antibodies before and after washing with DI water. Yellow selection denotes the area where surface fluorescence intensity values were taken. Black rough area at the right is the marked border area using Sharpie pens for mapping the exact location for consistency.

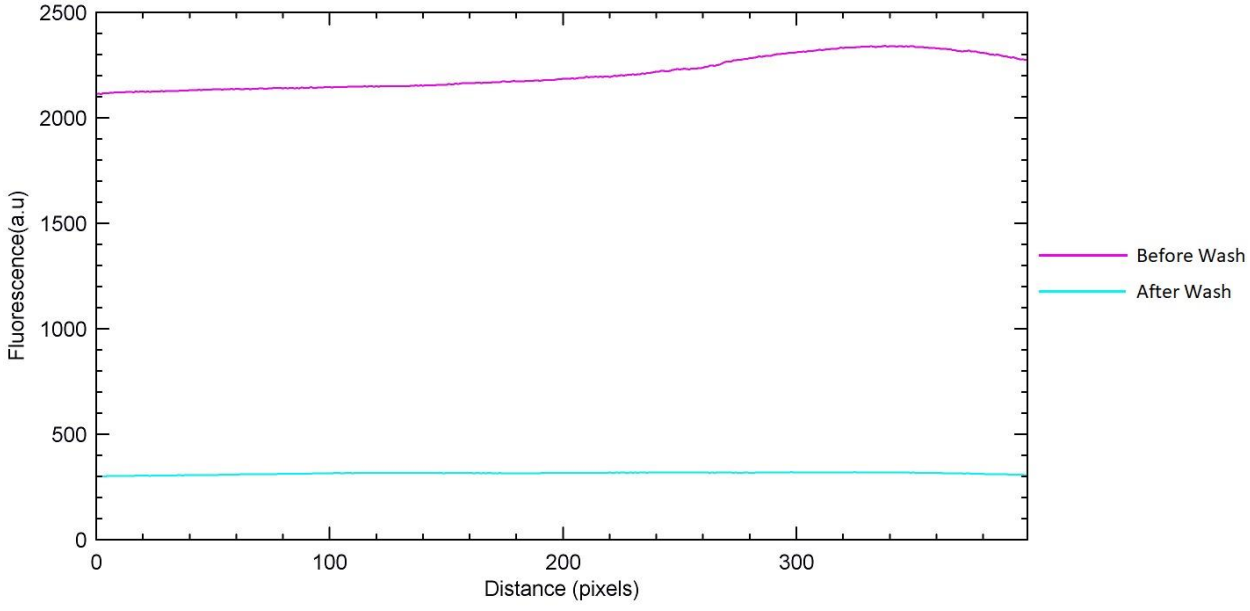

Figure 30. Fluorescence intensity values of antibodies on GO spin coated surface on glass before and wash with DI water.

d. Antibodies binding on PDMS surface only.

Fabricated PDMS stamps were cleaned thoroughly with IPA and compressed air to remove foreign bodies on the surface. Fluorescent antibodies (Anti-Human IgM Primary antibody) were drop casted on the PDMS surface with micro channels, allowed to incubate for 1 hour followed by DI water washing and then observed under the microscope. The fluorescence intensity values were taken from the antibodies functionalized spots on the PDMS surface. Intensity measurements were performed by Fiji software in the way described for GO surfaces.

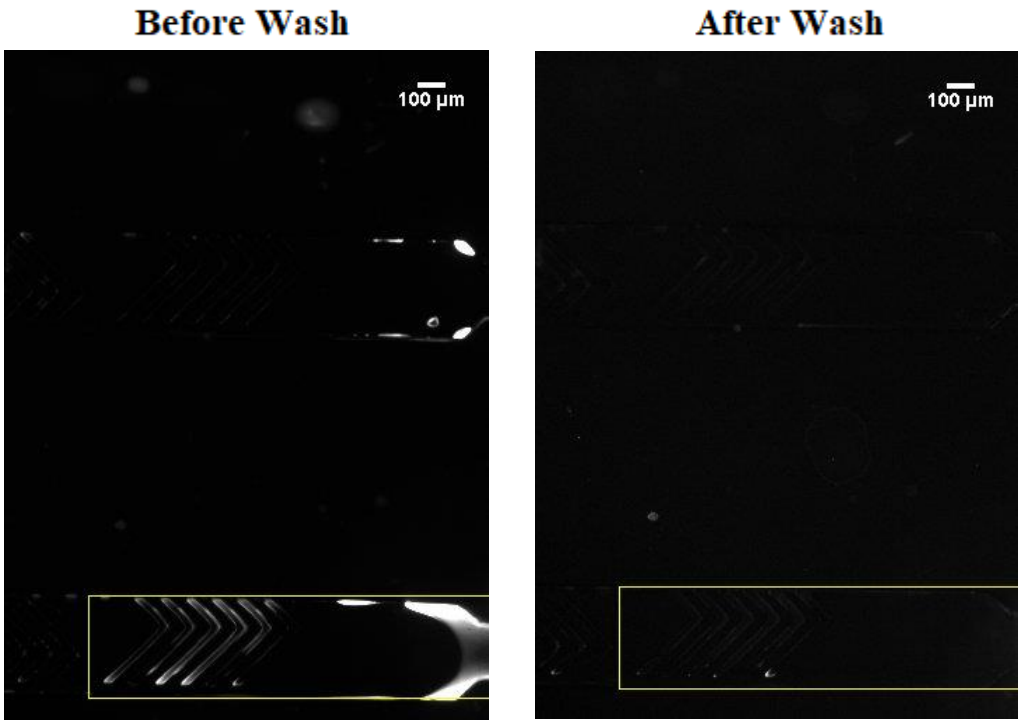

Figure 31. Fluorescence microscopy images of PDMS microchannels with antibodies before and after washing with DI water. Yellow selection denotes the area from where surface fluorescence intensity values were taken.

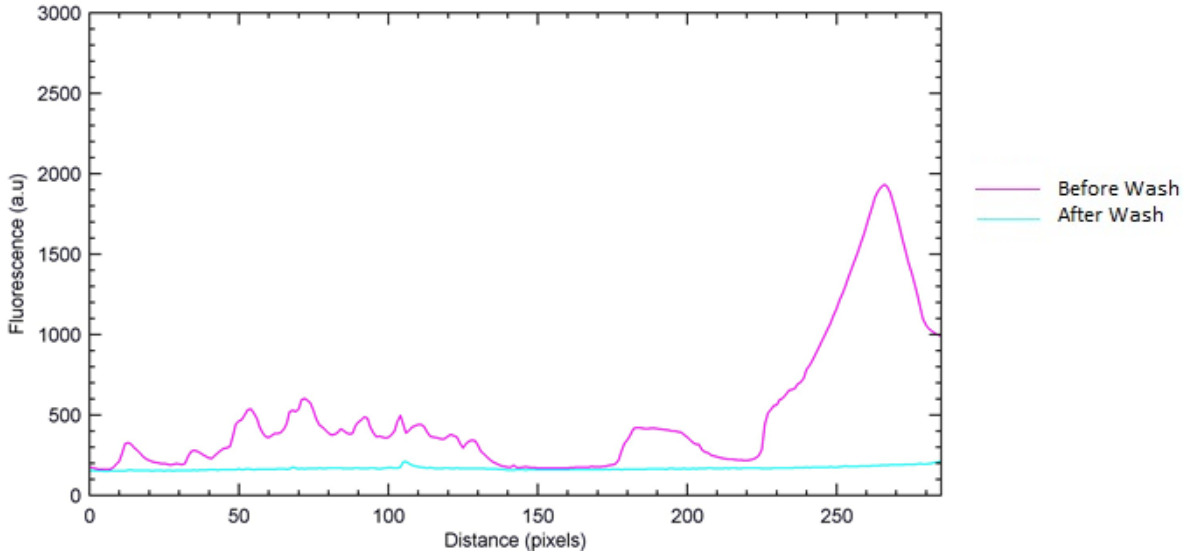

Figure 32. Fluorescence intensity values chart of antibodies on PDMS microchannel surface before and wash with DI water.

Average intensity values of the fluorescence signals from the four different surfaces were taken and the change in loss of fluorescence intensity values was calculated. We found that the binding (%) after washing away unbound fluorescent antibodies calculated from the fluorescence values in each surface were in decreasing order for PEG-GO spincoated glass, PEG-GO dropcasted on glass, PDMS only surfaces and plain glass surfaces without PEG-GO (Table 2). A net gain of ~23.17% of fluorescence signal intensity on the PEG-GO dropcasted on glass compared to the PDMS only surface demonstrated the PEG-GO's loading superiority over PDMS. This gain was even higher in the spin coated GO surface with a net gain of ~58.66% over PDMS, ~35.49% over dropcasted PEG-GO on glass and ~78.63% over a plain glass surface without PEG-GO. All these gain percent values are rounded to 4 significant figures. As the fluorescence signals originate from the antibodies, it could be seen that the PEG-GO functionalization definitely aids in the binding affinity of the antibodies towards the bioreceptors on the functionalized surfaces. Because nanomaterials like graphene oxide have a high surface to volume ratio, they provide multiple capture sites for properly functionalized and linked biomolecules as evident from the charts and images. The table below provides average columnar (vertical) fluorescence values scanned over a horizontal area before and after washing with a DPBS buffer solution for the four different surfaces discussed:

Table 2. Surface fluorescence values of fluorescent antibodies on different surfaces

	Substrate Surfaces	Average Surface Fluorescence Intensity values		
		Before Wash	After Wash	Average Binding(%)
1	PDMS without PEG-GO	489.1288397	167.1539303	34.17380386
2	PEG-GO dropcasted on Glass	813.1390225	466.3038978	57.34614683
3	Plain Glass surface without PEG-GO	2206.890314	313.4935204	14.20521529
4	Spincoated PEG-GO on Glass	356.2212699	330.7021825	92.83616967

While this is only a measurement of average columnar fluorescence intensity values across a known horizontal scanned area, it certainly shows an increased rate of capture antibodies loaded onto the graphene oxide surface. We intend to use other techniques to precisely measure the amount of antibodies and check the role of bacterial contamination and its impact on biomolecules surface in the near future. UV-vis spectroscopy might give more information on the precise amount of antibodies that is bound to various surfaces. After binding affinity tests, we tested these GO functionalized devices and non-functionalized devices with different cell lines to determine capture efficiencies of the system.

3.3 Cell isolation on GO functionalized and non-functionalized devices

GO functionalized and non-functionalized microfluidic devices were prepared for cell capture tests. DU145 prostate cancer cells were spiked in DPBS solution with 1% BSA. These were stained by UV excitable NucBlue™ Live ReadyProbes™ reagent for 30 minutes before flowing through the microfluidic devices. These probes contain DAPI, which tightly binds to the nucleus of the cell and gives a blue fluorescence when excited by UV light. Different flow rates based on previous rates used for capturing tumor cells with similar devices[13,27,49] were initially studied and tested. Flow rates between 3-5 µL/min gave optimal capture results after experimental observation. For cell capture count experiments, a flow rate of 5 /min was used. Flow rates beyond 50ul/min was too fast for target-receptor interactions. Flow rates below 3 µL/min would be too low for the biofluids to be pumped inside the channel possibly due to high resistance inside the channels.

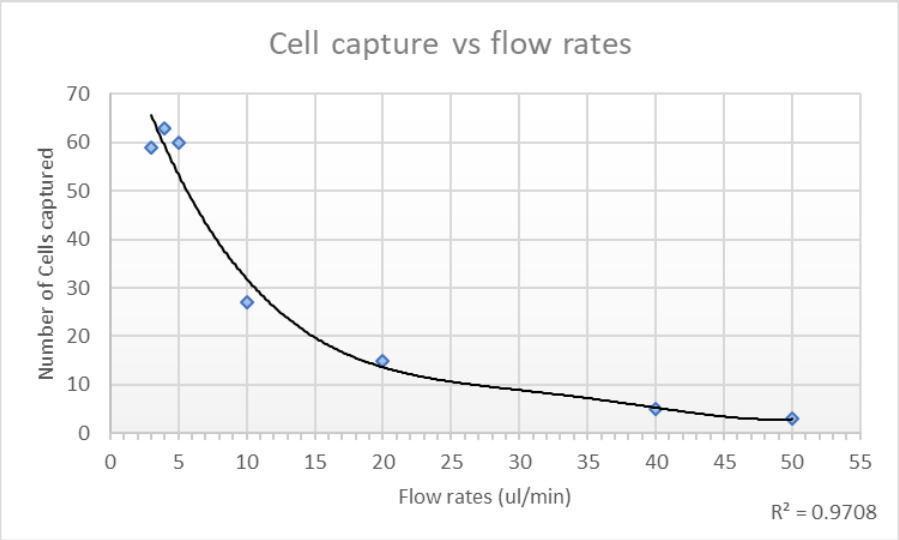

Figure 33. Cell capture counts vs flow rates in functionalized microfluidic devices. Trendline denotes a 3rd degree polynomial fit.

Briefly, the entire flow process for cell infusion and capture inside the device is described as follows:

1. DPBS was passed through the device at a flow rate of 100 µL/min for 10 minutes to remove any bubbles or foreign particles inside the chip.
2. GMBS was infused at 20 µL/min for 20 minutes followed by a 30 minutes incubation period.
3. Device was washed with DPBS flow at a flow rate of 50 µL/min for 2 minutes to clear any unbound GMBS molecules.
4. Streptavidin was introduced at a flow rate of 20 µL/min for a 1-hour incubation time.
5. Device was washed with DPBS at a flow rate of 50 µL/min for 5 minutes to clear unbound proteins.
6. MIL-38 antibodies were passed through the device at a flow rate of 20 µL/min for 10 minutes and was allowed for a 1-hour incubation period.

7. Device was washed again with DPBS at flow rate of 50 µL/min to remove unbound antibodies
8. DU145 cells (stained with NucBlue™ Live ReadyProbes™ reagents) were passed through the chip at a rate of 5 µL/min.
9. Captured cells were counted manually under the microscope through the computer screen in each channel.

These cell flow tests were performed for both GO functionalized and non-functionalized chips. The cell capture counts for both designs were recorded by visual observation through the screen. In most cases, nucleii of cells were visible and counting was made accurately. In cases where nucleii were not visible, cell measurements were taken with Fiji and cells above 5 microns were counted as 1 cell and below were not counted. Cell clustering is a known effect and blockers like BSA can be used to negate the effect however care should be taken as BSA can also raise false negatives in any system. Fig 34 and 35 show bright field and fluorescence images of captured cells inside microchannels

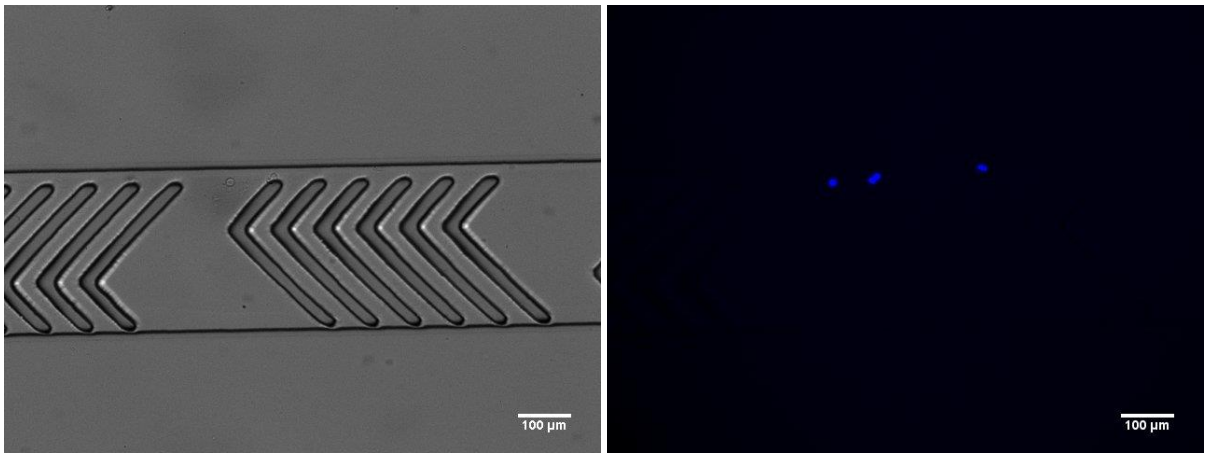

Figure 34. Bright field images of microchannels with DAPI stained cells isolated (left) and fluorescence microscopy images (Right).

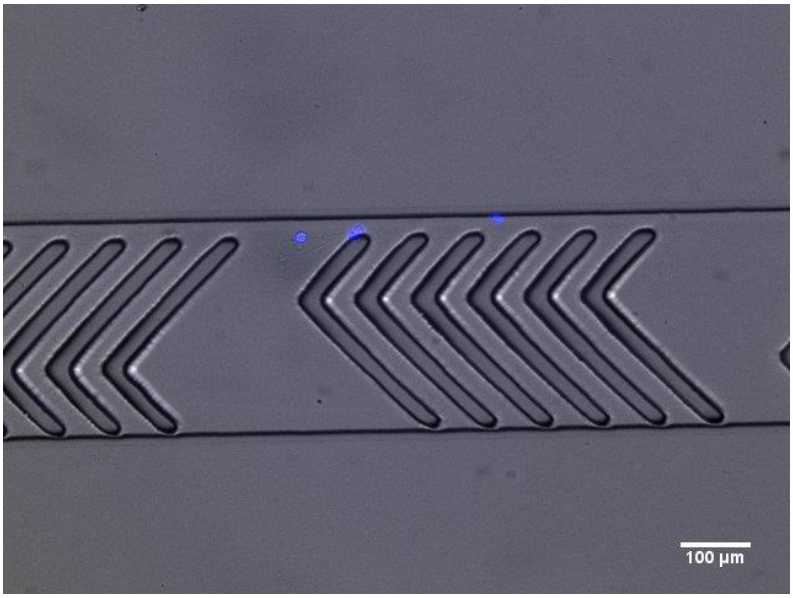

Figure 35. Composite merged image of Figure 35 left and right images giving the exact location of the isolated cells.

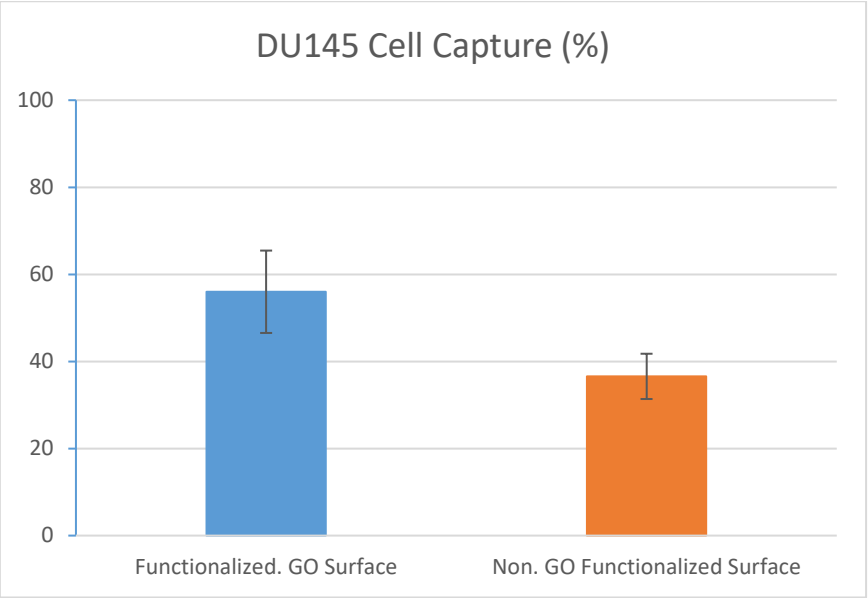

Figure 36. DU145 Cell Capture efficiency (%) on a GO functionalized vs non-GO functionalized microfluidic devices (n=5). Error bars represent the standard deviation from the average capture rate.

The average cell capture efficiency for DU145 cells on our GO functionalized microfluidic devices was ~56% compared to 36.6% on non-GO functionalized surfaces which showed a clear increase in capture rates of DU145 cells on GO functionalized surfaces. There was a 2.14% error in cell count (~3 cells) before infusion. This error rises from the initial counting error when syringing in the cells as some cells may remain on the specimen tube. A blocker solution like BSA can be used but this can raise false negatives on the device. The error value was calculated as a deviation percent from the mean value of the repeat counts of a known volume of cells on 96 well plates before and after syringing. This value related to the counting error up to the 'syringing in' point of the cells for flow inside the device. The capture efficiency we have reported we believe is lower to its true value as cells can also remain adhered on the infusing syringe and the tubing. This means the number of cells that passed through the device is most always slightly lower than the calculated number, which gives a lower capture rate than in reality as the efficiency is calculated as the captured cell count over a fixed total cell count.

Researchers have reported various capture rates and have acknowledged this negative as well as some reports of positive counting error throughout literature. For example some have reported over 100% value in some trials because of counting errors.[68] Cell capture efficiencies also depend on the specificity of the antibodies. Higher capture efficiencies are commonly reported for EpCAM expressing tumor lines, which are much more specific than the antibodies we have used. However, cell capture efficiency and counting or collecting outside the device is not the major component or in the future scope of this thesis work as we intend to continue on multi profiling of tumors and parallel detection of cell lines on chip.

3.4 MIL-38 specificity in GO functionalized microfluidic devices

C3 cells were spiked in DPBS solution with 1% Bovine Serum Albumin (BSA). These cells were used as the control line in our experiments as Mil-38 antibodies have very less affinity towards the C3 cells. We sought to verify the negligible affinity of the Mil-38 antibody towards the C3 cells. These were also stained by UV excitable NucBlue™ Live ReadyProbes™ Reagent for 30 minutes before flowing through the glass slides. The flow process used for capturing and counting these cells was the same as that used for the DU145 cells.

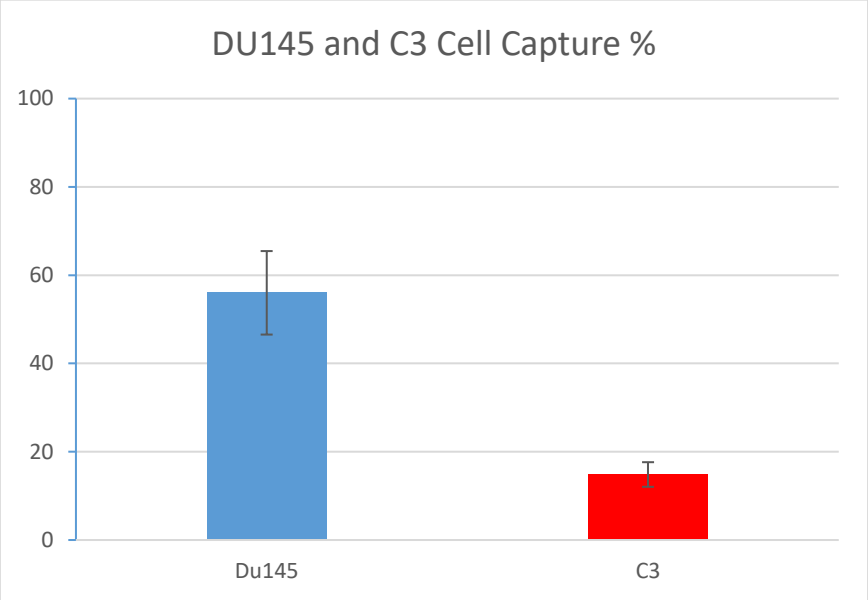

Figure 37. DU145 vs C3 cell Capture efficiency (%) on a GO functionalized microfluidic devices.

The average cell capture efficiency for C3 cells (Fig.38) on GO functionalized microfluidic devices was about 14.83 % compared to 56% for DU145 on the same GO surfaces which showed much less affinity of the antibody Mil-38 for the C3 cell line compared to DU145. Cell counting error percent was calculated in the same way used for DU145 cell counting. For the C3 cell line, there was a 2.5% error in cell count (~4 cells) before infusion. As expected, the results nonetheless demonstrated that our microfluidic chip does not increase nonspecific binding of cells, which can be an issue in biosensors. Negative cells can still bind to the receptors and the surface of the microfluidic chip due to the non-specific adsorption (NSA) condition that has been discussed earlier in the thesis. This would mean that in a real direct sample from a human, negative cells would also be present and would give false positive results. This can be corrected by staining the positive and negative cells with different dyes or fluorescent materials before infusing inside the microfluidic device.

Chapter 4.

Conclusions and Future perspectives

4.1 Summary and research outcomes

Circulating tumor cells are metastasizing cells that can circulate to distant sites where they make new colonies. These tumor cells can provide essential information regarding antigen expressions, stages of cancer and can be used as biomarkers in detection and therapeutic monitoring. However, these cells are very rare in early stages of cancer and their isolation and enrichment is valuable for the clinical community but also equally challenging. Microfluidic devices are widely used in current CTC isolation research. Nanomaterials have also found use for enhancing the performance of these microfluidic devices for capturing CTCs.

In this research, we used the nanomaterial graphene oxide to functionalize microfluidic devices based on glass substrates and PDMS micro-channels. We PEGylated the graphene oxide binding it to the glass surface and used the cross linker GMBS to bind one of its arms to the nanomaterial and the other to the binding protein. We chose Streptavidin as the binding protein to bind it to the cross linker and the capture antibodies. MIL-38 from Minomic® was used as the capture antibody to isolate DU145 and C3 cell lines. We then used our results to compare and contrast the capture efficiencies of our GO functionalized and non-functionalized microfluidic devices. Simultaneously, we also tested the binding affinities of antibodies on GO and non-GO surfaces to demonstrate the increased capture sites on GO surfaces before and after washing away the antibodies.

Firstly, the functionalizing materials needed before binding the devices were prepared. Graphene oxide was functionalized with PEG lipids and spin coated on glass surfaces and observed under SEM and AFM. Variations in uniformity and structural differences based on plasma treatment of surfaces were noted and these devices were allowed to incubate for a day before binding with fabricated PDMS microchannel embedded stamps for further experiments.

Secondly, the binding affinity of a fluorescent antibody (Anti-Human IgM) was tested on different surfaces with and without PEG-GO functionalization. Our results showed that graphene oxide functionalization on a surface increases the bound antibodies by increasing capture sites for the antibodies due to more bio-receptors anchored on the PEG-GO loaded surfaces. The average increase in binding affinity based on the fluorescence signal intensity (fluorescent IgM antibodies) was obtained as a cross sectional fluorescence value for the four different surfaces. The net gain of

fluorescence values from the antibodies was much higher on the spin coated PEG- GO surface with its average gain of ~58.66% over PDMS only surface, ~35.49% over drop casted PEG-GO on glass and ~78.631% over plain glass surface without PEG-GO.

Thirdly, the bonded microfluidic devices with GO functionalized glass surface and non-functionalized surfaces were prepared for microflows of bioreceptors and cell lines. First, GMBS, the cross-linking agent we used to bind the GO sheets with the binding protein was introduced and allowed to incubate. Unbound cross-linking molecules were washed away with ethanol. Then, Streptavidin, which is a binding protein, was introduced inside the devices and allowed to incubate. Unbound proteins were washed away with DPBS and finally the capture antibodies were flown to bind them to the proteins and create capture sites for tumor cell lines. After an incubation period, DPBS was flown to wash away unbound antibodies. DU145 and C3 cell lines, spiked in buffer solution DPBS were introduced to both types of microfluidic devices at flow rates mentioned in the results and their capture efficiencies were observed and noted based on DAPI fluorescence signals from the cell nucleus.

We discovered out that GO functionalized microfluidic devices had a capture efficiency of ~56% compared to 36.6% on non-GO devices for DU145 cells. To demonstrate the specificity of the antibody itself, we used C3 cell lines as negative control for the experiments on GO functionalized devices. The capture efficiencies for C3 cell lines on GO devices were ~14.83%, which is a significant drop on capture rates, but this is an expected result as MIL-38 is more highly specific to DU145 cells. While the capture efficiencies for DU145 cell lines on the microfluidic devices is lower than many other devices, we point out that this might be the result of cell counting errors. We calculated error percent in cell counts up to the point of syringing before infusion by repeated cell counts of a known volume of cells on 96 well plates by taking the cells in and out through a syringe. The error percent of DU145 and C3 cells for this process was about 2.14% and 2.5% respectively. Some cells can be adhered in the tubing and the syringe itself after infusion. We were not able to quantify these errors, and this can affect the results giving false negative capture efficiencies. Nonetheless, cell counting was not a major theme of this project and we demonstrated that GO surfaces increased capture efficiencies on our microfluidic devices compared to a plain surface based microfluidic device. These devices will be used further for multiple profiling of tumor cell lines through techniques like Surface Enhanced Raman spectroscopy (SERS).

Our approach of functionalizing nanomaterials on microfluidic devices certainly aids in isolation and capture efficiency of CTCs. Affinity based capture methods possess the cellular heterogeneity issue for which GO functionalized microfluidic device can be used as a solution. Different antibodies can be coated on these devices by washing off in each cycle which can introduce different capture sites

for different cells inside the same device. There will always be the error due to the non-specific adsorption of biomolecules that remains a challenge with this as well as any other techniques. Fabrication complexity is not a major issue with the device we have developed as graphene oxide coating was achieved with simple spin coating methods. Microfluidic device and design fabrication can be complex but once a master mold has been designed, this complexity is made simple. This technique has a higher throughput compared to other techniques and does not require complex devices and equipment that may be needed for other methods.

4.2 Future works

In this research work, cell lines were spiked on buffer solution DPBS. In real conditions, a blood sample has to be used as the medium for capture efficiencies tests. We intend to use both artificial blood as well as direct patient samples in the future in our microfluidic devices to demonstrate capturing of tumor cell lines inside the devices. To correct the infusion errors, we aim to use a microelectrode-based flow cell system like the one developed by PINE® research company which is an integrated flow system that minimizes the common infusion errors in lab based flow cell systems. With this system, cells will be in constant rotation inside the device and will have minimal chances of having non-specific adhesion inside the infusion devices.

For the quantification of binding affinities of antibodies, we will perform repeat fluorescence intensity tests on the same surface before and after functionalization. Considering the limited time period for this masters research project, this was not possible to achieve and present in this thesis. We also aim to use techniques like UV-Vis spectroscopy to get the precise amount of biomolecules on a given surface before and after washing unbound molecules.

Finally, as part of a future PhD work that will be conducted based on this thesis work, we will focus our efforts on detection technologies for CTCs on chip and parallel profiling of tumors on the same chip through techniques like SERS.

References

1 Kim, M. Y. *et al.* Tumor Self-Seeding by Circulating Cancer Cells. *Cell* **139**, 1315-1326, doi:10.1016/j.cell.2009.11.025 (2009).

2 Pantel, K. & Speicher, M. R. The biology of circulating tumor cells. *Oncogene* **35**, 1216-1224, doi:10.1038/onc.2015.192 (2016).

3 Patil, P. U., D'Ambrosio, J., Inge, L. J., Mason, R. W. & Rajasekaran, A. K. Carcinoma cells induce lumen filling and EMT in epithelial cells through soluble E-cadherin-mediated activation of EGFR. *J Cell Sci* **128**, 4366-4379, doi:10.1242/jcs.173518 (2015).

4 Nabet, B. Y. *et al.* Exosome RNA Unshielding Couples Stromal Activation to Pattern Recognition Receptor Signaling in Cancer. *Cell* **170**, 352-+, doi:10.1016/j.cell.2017.06.031 (2017).

5 Cristofanilli, M. *et al.* Circulating tumor cells, disease progression, and survival in metastatic breast cancer. *New Engl J Med* **351**, 781-791, doi:DOI 10.1056/NEJMoa040766 (2004).

6 Harouaka, R., Kang, Z., Zheng, S. Y. & Cao, L. Circulating tumor cells: advances in isolation and analysis, and challenges for clinical applications. *Pharmacol Ther* **141**, 209-221, doi:10.1016/j.pharmthera.2013.10.004 (2014).

7 Rawal, S., Yang, Y. P., Cote, R. & Agarwal, A. Identification and Quantitation of Circulating Tumor Cells. *Annu Rev Anal Chem (Palo Alto Calif)* **10**, 321-343, doi:10.1146/annurev-anchem-061516-045405 (2017).

8 Hyun, K. A., Kim, J., Gwak, H. & Jung, H. I. Isolation and enrichment of circulating biomarkers for cancer screening, detection, and diagnostics. *Analyst* **141**, 382-392, doi:10.1039/c5an01762a (2016).

9 Krebs, M. G. *et al.* Evaluation and Prognostic Significance of Circulating Tumor Cells in Patients With Non-Small-Cell Lung Cancer. *J Clin Oncol* **29**, 1556-1563, doi:10.1200/Jco.2010.28.7045 (2011).

10 Ma, Y. H. V., Middleton, K., You, L. D. & Sun, Y. A review of microfluidic approaches for investigating cancer extravasation during metastasis. *Microsyst Nanoeng* **4**, doi:UNSP 1710410.1038/micronano.2017.104 (2018).

11 Murlidhar, V., Rivera-Baez, L. & Nagrath, S. Affinity Versus Label-Free Isolation of Circulating Tumor Cells: Who Wins? *Small* **12**, 4450-4463, doi:10.1002/smll.201601394 (2016).

12 Kozminsky, M., Wang, Y. & Nagrath, S. The incorporation of microfluidics into circulating tumor cell isolation for clinical applications. *Curr Opin Chem Eng* **11**, 59-66, doi:10.1016/j.coche.2016.01.005 (2016).

13 Yoon, H. J. *et al.* Sensitive capture of circulating tumour cells by functionalized graphene oxide nanosheets. *Nat Nanotechnol* **8**, 735-741, doi:10.1038/nnano.2013.194 (2013).

14 Williams, S. C. P. Circulating tumor cells. *P Natl Acad Sci USA* **110**, 4861-4861, doi:10.1073/pnas.1304186110 (2013).

15 Sporn, M. B. The war on cancer. *Lancet* **347**, 1377-1381, doi:Doi 10.1016/S0140-6736(96)91015-6 (1996).

16 Weiss, L. Observations on the antiquity of cancer and metastasis. *Cancer Metast Rev* **19**, 193-204, doi:Doi 10.1023/A:1010646304844 (2000).

17 Wittekind, C. & Neid, M. Cancer invasion and metastasis. *Oncology-Basel* **69**, 14-16, doi:10.1159/000086626 (2005).

18 Alix-Panabieres, C. & Pantel, K. Technologies for detection of circulating tumor cells: facts and vision. *Lab Chip* **14**, 57-62, doi:10.1039/c3lc50644d (2014).

19 Autebert, J. *et al.* High purity microfluidic sorting and analysis of circulating tumor cells: towards routine mutation detection. *Lab Chip* **15**, 2090-2101, doi:10.1039/c5lc00104h (2015).

20 Cheng, I. F. *et al.* Antibody-free isolation of rare cancer cells from blood based on 3D lateral dielectrophoresis. *Lab Chip* **15**, 2950-2959, doi:10.1039/c5lc00120j (2015).

21 Costa, C., Abal, M., Lopez-Lopez, R. & Muinelo-Romay, L. Biosensors for the detection of circulating tumour cells. *Sensors (Basel)* **14**, 4856-4875, doi:10.3390/s140304856 (2014).

22 Nagrath, S. *et al.* Isolation of rare circulating tumour cells in cancer patients by microchip technology. *Nature* **450**, 1235-1239, doi:10.1038/nature06385 (2007).

23 Qian, W., Zhang, Y. & Chen, W. Capturing Cancer: Emerging Microfluidic Technologies for the Capture and Characterization of Circulating Tumor Cells. *Small* **11**, 3850-3872, doi:10.1002/smll.201403658 (2015).
24 Murlidhar, V. *et al.* A radial flow microfluidic device for ultra-high-throughput affinity-based isolation of circulating tumor cells. *Small* **10**, 4895-4904, doi:10.1002/smll.201400719 (2014).
25 Murlidhar, V., Ramnath, N., Nagrath, S. & Reddy, R. M. Optimizing the Detection of Circulating Markers to Aid in Early Lung Cancer Detection. *Cancers* **8**, doi:ARTN 6110.3390/cancers8070061 (2016).
26 Wan, Y. *et al.* Nanotextured substrates with immobilized aptamers for cancer cell isolation and cytology. *Cancer* **118**, 1145-1154, doi:10.1002/cncr.26349 (2012).
27 Hyun, K. A., Lee, T. Y. & Jung, H. I. Negative enrichment of circulating tumor cells using a geometrically activated surface interaction chip. *Anal Chem* **85**, 4439-4445, doi:10.1021/ac3037766 (2013).
28 Lin, M. *et al.* Nanostructure embedded microchips for detection, isolation, and characterization of circulating tumor cells. *Acc. Chem. Res.* **47**, 2941-2950, doi:10.1021/ar5001617 (2014).
29 Jin, C. *et al.* Technologies for label-free separation of circulating tumor cells: from historical foundations to recent developments. *Lab Chip* **14**, 32-44, doi:10.1039/c3lc50625h (2014).
30 Zborowski, M. & Chamers, J. J. Rare Cell Separation and Analysis by Magnetic Sorting. *Anal Chem* **83**, 8050-8056, doi:10.1021/ac200550d (2011).
31 Gascoyne, P. R. & Shim, S. Isolation of circulating tumor cells by dielectrophoresis. *Cancers (Basel)* **6**, 545-579, doi:10.3390/cancers6010545 (2014).
32 Li, P. *et al.* Acoustic separation of circulating tumor cells. *P Natl Acad Sci USA* **112**, 4970-4975, doi:10.1073/pnas.1504484112 (2015).
33 Krebs, M. G. *et al.* Analysis of Circulating Tumor Cells in Patients with Non-small Cell Lung Cancer Using Epithelial Marker-Dependent and -Independent Approaches. *J Thorac Oncol* **7**, 306-315, doi:10.1097/JTO.0b013e31823c5c16 (2012).
34 Takahashi, K., Hattori, A., Suzuki, I., Ichiki, T. & Yasuda, K. Non-destructive on-chip cell sorting system with real-time microscopic image processing. *J Nanobiotechnology* **2**, 5, doi:10.1186/1477-3155-2-5 (2004).
35 Krebs, M. G., Hou, J. M., Ward, T. H., Blackhall, F. H. & Dive, C. Circulating tumour cells: their utility in cancer management and predicting outcomes. *Ther Adv Med Oncol* **2**, 351-365, doi:10.1177/1758834010378414 (2010).
36 Syverud, B. C., Lin, E., Nagrath, S. & Larkin, L. M. Label-Free, High-Throughput Purification of Satellite Cells Using Microfluidic Inertial Separation. *Tissue Eng Part C Methods* **24**, 32-41, doi:10.1089/ten.TEC.2017.0316 (2018).
37 Ohnaga, T. *et al.* Capture of esophageal and breast cancer cells with polymeric microfluidic devices for CTC isolation. *Mol Clin Oncol* **4**, 599-602, doi:10.3892/mco.2016.734 (2016).
38 Sayyadi, N. *et al.* Sensitive Time-Gated Immunoluminescence Detection of Prostate Cancer Cells Using a TEGylated Europium Ligand. *Anal Chem* **88**, 9564-9571, doi:10.1021/acs.analchem.6b02191 (2016).
39 Tabeling, P. *Introduction to microfluidics*. (Oxford University Press on Demand, 2005).
40 Whitesides, G. M. The origins and the future of microfluidics. *Nature* **442**, 368, doi:10.1038/nature05058 (2006).
41 ELVESYS®. in *Online Content* (2015).
42 Chhabra, R. P. Non-Newtonian Fluids: An Introduction. *Rheology of Complex Fluids*, 3-34, doi:10.1007/978-1-4419-6494-6_1 (2010).
43 Ward, K. & Fan, Z. H. Mixing in microfluidic devices and enhancement methods. *J Micromech Microeng* **25**, doi:Artn 09400110.1088/0960-1317/25/9/094001 (2015).
44 Lee, C. Y., Chang, C. L., Wang, Y. N. & Fu, L. M. Microfluidic Mixing: A Review. *Int J Mol Sci* **12**, 3263-3287, doi:10.3390/ijms12053263 (2011).
45 Green, J., Holdo, A. E. & Khan, A. A review of passive and active mixing systems in microfluidic devices. *Int J Multiphysics* **1**, 1-32, doi:Doi 10.1260/175095407780130544 (2007).

46 Mansur, E. A., Ye, M. X., Wang, Y. D. & Dai, Y. Y. A state-of-the-art review of mixing in microfluidic mixers. *Chinese J Chem Eng* **16**, 503-516, doi:Doi 10.1016/S1004-9541(08)60114-7 (2008).
47 Capretto, L., Cheng, W., Hill, M. & Zhang, X. L. Micromixing Within Microfluidic Devices. *Top Curr Chem* **304**, 27-68, doi:10.1007/128_2011_150 (2011).
48 Zahn, J. D. & Fok, A. Micromixing Within Microfluidic Devices. *Artech Hse Meth Bioe*, 59-81 (2010).
49 Stott, S. L. *et al.* Isolation of circulating tumor cells using a microvortex-generating herringbone-chip. *P Natl Acad Sci USA* **107**, 18392-18397, doi:10.1073/pnas.1012539107 (2010).
50 Stroock, A. D. *et al.* Chaotic mixer for microchannels. *Science* **295**, 647-651, doi:DOI 10.1126/science.1066238 (2002).
51 McDonald, J. C. *et al.* Fabrication of microfluidic systems in poly(dimethylsiloxane). *Electrophoresis* **21**, 27-40, doi:Doi 10.1002/(Sici)1522-2683(20000101)21:1<27::Aid-Elps27>3.0.Co;2-C (2000).
52 Thorsen, T., Maerkl, S. J. & Quake, S. R. Microfluidic large-scale integration. *Science* **298**, 580-584, doi:10.1126/science.1076996 (2002).
53 O'Neill, P. F. *et al.* Advances in three-dimensional rapid prototyping of microfluidic devices for biological applications. *Biomicrofluidics* **8**, 052112, doi:10.1063/1.4898632 (2014).
54 Shields, C. W. t., Reyes, C. D. & Lopez, G. P. Microfluidic cell sorting: a review of the advances in the separation of cells from debulking to rare cell isolation. *Lab Chip* **15**, 1230-1249, doi:10.1039/c4lc01246a (2015).
55 Deller, M. C. & Rupp, B. Approaches to automated protein crystal harvesting. *Acta Crystallogr F* **70**, 133-155, doi:10.1107/S2053230x14000387 (2014).
56 Eastburn, D. J. *et al.* Microfluidic droplet enrichment for targeted sequencing. *Nucleic Acids Res* **43**, e86, doi:10.1093/nar/gkv297 (2015).
57 Huang, Q. *et al.* Nanotechnology-Based Strategies for Early Cancer Diagnosis Using Circulating Tumor Cells as a Liquid Biopsy. *Nanotheranostics* **2**, 21-41, doi:10.7150/ntno.22091 (2018).
58 Pumera, M. Nanomaterials meet microfluidics. *Chem Commun* **47**, 5671-5680, doi:10.1039/c1cc11060h (2011).
59 Yujun, S., Josef, H. & R., K. C. S. S. Microfluidic Synthesis of Nanomaterials. *Small* **4**, 698-711, doi:doi:10.1002/smll.200701029 (2008).
60 Wang, L., Asghar, W., Demirci, U. & Wan, Y. Nanostructured substrates for isolation of circulating tumor cells. *Nano today* **8**, 347-387 (2013).
61 Park, G. S. *et al.* Full surface embedding of gold clusters on silicon nanowires for efficient capture and photothermal therapy of circulating tumor cells. *Nano letters* **12**, 1638-1642, doi:10.1021/nl2045759 (2012).
62 Wang, S. *et al.* Highly efficient capture of circulating tumor cells by using nanostructured silicon substrates with integrated chaotic micromixers. *Angew. Chem. (International ed. in English)* **50**, 3084-3088, doi:10.1002/anie.201005853 (2011).
63 Zhao, L. *et al.* High-purity prostate circulating tumor cell isolation by a polymer nanofiber-embedded microchip for whole exome sequencing. *Adv Mater* **25**, 2897-2902, doi:10.1002/adma.201205237 (2013).
64 Hou, S. *et al.* Polymer nanofiber-embedded microchips for detection, isolation, and molecular analysis of single circulating melanoma cells. *Angew. Chem. (International ed. in English)* **52**, 3379-3383, doi:10.1002/anie.201208452 (2013).
65 Wen, C.-Y. *et al.* Quick-Response Magnetic Nanospheres for Rapid, Efficient Capture and Sensitive Detection of Circulating Tumor Cells. *Acs Nano* **8**, 941-949, doi:10.1021/nn405744f (2014).
66 Liu, H. *et al.* Hydrophobic interaction-mediated capture and release of cancer cells on thermoresponsive nanostructured surfaces. *Adv Mater* **25**, 922-927, doi:10.1002/adma.201203826 (2013).
67 Earhart, C. M. *et al.* Isolation and mutational analysis of circulating tumor cells from lung cancer patients with magnetic sifters and biochips. *Lab Chip* **14**, 78-88, doi:10.1039/c3lc50580d (2014).
68 Park, M. H. *et al.* Enhanced Isolation and Release of Circulating Tumor Cells Using Nanoparticle Binding and Ligand Exchange in a Microfluidic Chip. *J Am Chem Soc* **139**, 2741-2749, doi:10.1021/jacs.6b12236 (2017).

69 Kanchanapally, R., Fan, Z., Singh, A. K., Sinha, S. S. & Ray, P. C. Multifunctional hybrid graphene oxide for label-free detection of malignant melanoma from infected blood. *Journal of Materials Chemistry B* **2**, 1934-1937, doi:10.1039/C3TB21756F (2014).
70 Fan, Z., Senapati, D., Singh, A. K. & Ray, P. C. Theranostic Magnetic Core–Plasmonic Shell Star Shape Nanoparticle for the Isolation of Targeted Rare Tumor Cells from Whole Blood, Fluorescence Imaging, and Photothermal Destruction of Cancer. *Molecular Pharmaceutics* **10**, 857-866, doi:10.1021/mp300468q (2013).
71 Bardhan, N. M. *et al.* Enhanced Cell Capture on Functionalized Graphene Oxide Nanosheets through Oxygen Clustering. *Acs Nano* **11**, 1548-1558, doi:10.1021/acsnano.6b06979 (2017).
72 Chen, G. Y. *et al.* Graphene Oxide Nanosheets Modified with Single-Domain Antibodies for Rapid and Efficient Capture of Cells. *Chem-Eur J* **21**, 17178-17183, doi:10.1002/chem.201503057 (2015).
73 Zhang, Y. B., Tan, Y. W., Stormer, H. L. & Kim, P. Experimental observation of the quantum Hall effect and Berry's phase in graphene. *Nature* **438**, 201-204, doi:10.1038/nature04235 (2005).
74 Novoselov, K. S. *et al.* Two-dimensional gas of massless Dirac fermions in graphene. *Nature* **438**, 197-200, doi:10.1038/nature04233 (2005).
75 Stankovich, S. *et al.* Graphene-based composite materials. *Nature* **442**, 282-286, doi:10.1038/nature04969 (2006).
76 Lee, C., Wei, X. D., Kysar, J. W. & Hone, J. Measurement of the elastic properties and intrinsic strength of monolayer graphene. *Science* **321**, 385-388, doi:10.1126/science.1157996 (2008).
77 Luo, J. Y. *et al.* Graphene Oxide Nanocolloids. *J Am Chem Soc* **132**, 17667-17669, doi:10.1021/ja1078943 (2010).
78 Loh, K. P., Bao, Q. L., Eda, G. & Chhowalla, M. Graphene oxide as a chemically tunable platform for optical applications. *Nature Chemistry* **2**, 1015-1024, doi:10.1038/Nchem.907 (2010).
79 Zheng, Q. B., Li, Z. G., Yang, J. H. & Kim, J. K. Graphene oxide-based transparent conductive films. *Prog Mater Sci* **64**, 200-247, doi:10.1016/j.pmatsci.2014.03.004 (2014).
80 Geim, A. K. & Novoselov, K. S. The rise of graphene. *Nat Mater* **6**, 183-191, doi:DOI 10.1038/nmat1849 (2007).
81 Stankovich, S. *et al.* Synthesis of graphene-based nanosheets via chemical reduction of exfoliated graphite oxide. *Carbon* **45**, 1558-1565, doi:10.1016/j.carbon.2007.02.034 (2007).
82 Wang, Y., Shao, Y. Y., Matson, D. W., Li, J. H. & Lin, Y. H. Nitrogen-Doped Graphene and Its Application in Electrochemical Biosensing. *Acs Nano* **4**, 1790-1798, doi:10.1021/nn100315s (2010).
83 Zhu, Y. W. *et al.* Graphene and Graphene Oxide: Synthesis, Properties, and Applications. *Adv Mater* **22**, 3906-3924, doi:10.1002/adma.201001068 (2010).
84 Kumar, R. *et al.* Bulk synthesis of highly conducting graphene oxide with long range ordering. *Rsc Adv* **5**, 35893-35898, doi:10.1039/c5ra01943e (2015).
85 Song, Y. J., Qu, K. G., Zhao, C., Ren, J. S. & Qu, X. G. Graphene Oxide: Intrinsic Peroxidase Catalytic Activity and Its Application to Glucose Detection. *Adv Mater* **22**, 2206-2210, doi:10.1002/adma.200903783 (2010).
86 Wu, L. *et al.* A graphene-based chemical nose/tongue approach for the identification of normal, cancerous and circulating tumor cells. *Npg Asia Mater* **9**, doi:10.1038/am.2017.11 (2017).
87 Bianco, A., Kostarelos, K. & Prato, M. Applications of carbon nanotubes in drug delivery. *Curr Opin Chem Biol* **9**, 674-679, doi:10.1016/j.cbpa.2005.10.006 (2005).
88 Zhu, H., Yan, J. & Revzin, A. Catch and release cell sorting: electrochemical desorption of T-cells from antibody-modified microelectrodes. *Colloids Surf B Biointerfaces* **64**, 260-268, doi:10.1016/j.colsurfb.2008.02.010 (2008).
89 Li, S. S., He, H., Jiao, Q. C. & Chuong, P. H. Applications of Carbon Nanotubes in Drug and Gene Delivery. *Prog Chem* **20**, 1798-1803 (2008).
90 Sun, X. M. *et al.* Nano-Graphene Oxide for Cellular Imaging and Drug Delivery. *Nano Res* **1**, 203-212, doi:10.1007/s12274-008-8021-8 (2008).
91 Zhang, W. X., Zhang, Z. Z. & Zhang, Y. G. The application of carbon nanotubes in target drug delivery systems for cancer therapies. *Nanoscale Res Lett* **6**, doi:Artn 55510.1186/1556-276x-6-555 (2011).
92 Rafiee, J. *et al.* Wetting transparency of graphene. *Nat Mater* **11**, 217-222, doi:10.1038/Nmat3228 (2012).

93 Dreyer, D. R., Park, S., Bielawski, C. W. & Ruoff, R. S. The chemistry of graphene oxide. *Chem Soc Rev* **39**, 228-240, doi:10.1039/b917103g (2010).
94 Liu, Z., Robinson, J. T., Sun, X. M. & Dai, H. J. PEGylated nanographene oxide for delivery of water-insoluble cancer drugs. *J Am Chem Soc* **130**, 10876-+, doi:10.1021/ja803688x (2008).
95 Yoon, H. J. *et al.* Tunable Thermal-Sensitive Polymer-Graphene Oxide Composite for Efficient Capture and Release of Viable Circulating Tumor Cells. *Adv Mater* **28**, 4891-4897, doi:10.1002/adma.201600658 (2016).
96 Li, Y. Y. *et al.* Antibody-Modified Reduced Graphene Oxide Films with Extreme Sensitivity to Circulating Tumor Cells. *Adv Mater* **27**, 6848-+, doi:10.1002/adma.201502615 (2015).
97 Nellore, B. P. V. *et al.* Aptamer-Conjugated Graphene Oxide Membranes for Highly Efficient Capture and Accurate Identification of Multiple Types of Circulating Tumor Cells. *Bioconjugate Chem* **26**, 235-242, doi:10.1021/bc500503e (2015).
98 Gleghorn, J. P. *et al.* Capture of circulating tumor cells from whole blood of prostate cancer patients using geometrically enhanced differential immunocapture (GEDI) and a prostate-specific antibody. *Lab Chip* **10**, 27-29, doi:10.1039/b917959c (2010).
99 Adams, A. A. *et al.* Highly efficient circulating tumor cell isolation from whole blood and label-free enumeration using polymer-based microfluidics with an integrated conductivity sensor. *J Am Chem Soc* **130**, 8633-8641, doi:10.1021/ja8015022 (2008).
100 Saliba, A. E. *et al.* Microfluidic sorting and multimodal typing of cancer cells in self-assembled magnetic arrays. *Proc Natl Acad Sci U S A* **107**, 14524-14529, doi:10.1073/pnas.1001515107 (2010).
101 Yu, X. *et al.* Magneto-controllable capture and release of cancer cells by using a micropillar device decorated with graphite oxide-coated magnetic nanoparticles. *Small* **9**, 3895-3901, doi:10.1002/smll.201300169 (2013).
102 Ye Xu, J. A. P., Jilin Yan, Qingge Li, Z. Hugh Fan, and Weihong Tan. <Aptamer-Based Microfluidic Device for Enrichment,Sorting and detction of multiple cancer cells.pdf>. (2009).
103 Zhou, M. D. *et al.* Separable bilayer microfiltration device for viable label-free enrichment of circulating tumour cells. *Sci Rep* **4**, 7392, doi:10.1038/srep07392 (2014).
104 Shen, Q. *et al.* Specific capture and release of circulating tumor cells using aptamer-modified nanosubstrates. *Adv Mater* **25**, 2368-2373, doi:10.1002/adma.201300082 (2013).
105 Warkiani, M. E. *et al.* Slanted spiral microfluidics for the ultra-fast, label-free isolation of circulating tumor cells. *Lab Chip* **14**, 128-137, doi:10.1039/c3lc50617g (2014).
106 Hyun, K. A., Kwon, K., Han, H., Kim, S. I. & Jung, H. I. Microfluidic flow fractionation device for label-free isolation of circulating tumor cells (CTCs) from breast cancer patients. *Biosens Bioelectron* **40**, 206-212, doi:10.1016/j.bios.2012.07.021 (2013).
107 Lee, S. K. *et al.* Nanowire substrate-based laser scanning cytometry for quantitation of circulating tumor cells. *Nano letters* **12**, 2697-2704, doi:10.1021/nl2041707 (2012).
108 Chen, W. *et al.* Nanoroughened surfaces for efficient capture of circulating tumor cells without using capture antibodies. *Acs Nano* **7**, 566-575, doi:10.1021/nn304719q (2013).
109 Kwak, B. *et al.* Spiral shape microfluidic channel for selective isolating of heterogenic circulating tumor cells. *Biosensors and Bioelectronics* **101**, 311-316, doi:https://doi.org/10.1016/j.bios.2017.10.036 (2018).
110 Wang, X. B. *et al.* Cell separation by dielectrophoretic field-flow-fractionation. *Anal Chem* **72**, 832-839 (2000).
111 Ozkumur, E. *et al.* Inertial focusing for tumor antigen-dependent and -independent sorting of rare circulating tumor cells. *Sci Transl Med.* **5**, 179ra147, doi:10.1126/scitranslmed.3005616 (2013).
112 Truong, Q. *et al.* Glypican-1 as a Biomarker for Prostate Cancer: Isolation and Characterization. *J Cancer* **7**, 1002-1009, doi:10.7150/jca.14645 (2016).
113 Chen, Y. Y. *et al.* Capture and Identification of Heterogeneous Circulating Tumor Cells Using Transparent Nanomaterials and Quantum Dots-Based Multiplexed Imaging. *J Cancer* **7**, 69-79, doi:10.7150/jca.12722 (2016).
114 Massoner, P. *et al.* EpCAM is overexpressed in local and metastatic prostate cancer, suppressed by chemotherapy and modulated by MET-associated miRNA-200c/205. *Br J Cancer* **111**, 955-964, doi:10.1038/bjc.2014.366 (2014).

115 Guo, Y. L. *et al.* General Route toward Patterning of Graphene Oxide by a Combination of Wettability Modulation and Spin-Coating. *Acs Nano* **4**, 5749-5754, doi:10.1021/nn101463j (2010).

List of Acronyms

AFM	Atomic Force Microscopy
CTC	Circulating tumor cells
DI	De-ionized
DMSO	Dimethyl Sulfoxide
DSPE-PEG	1,2-distearoyl-sn-glycero-3-phosphoethanolamine-N-[amino(polyethylene glycol)-2000]
EpCAM	Epithelial cell adhesion molecule
GPC-1	Glypican-1
GMBS	N-(Gamma-Maleimidobutyryloxy) Succinimide
GO	Graphene Oxide
HB	Herringbone
IgM	Immunoglobulin M
NSA	Non specific adsorption
PDMS	Polydimethylsiloxane
PEG	Polyethylene Glycol
SAM	Self assembled monolayer
SEM	Scanning Electron Microscopy

The following 4 pages of the appendix removed from full access at the request of the author (Copyright holder). 2.9.2019

A3. Cell culture protocols (Fully done and provided by Victoria wang)

1. Pre-warm PBS, trypsin (from drawer) and medium (from fridge) in water bath (35℃) for 20 mins. (Put three of them back to places when all finished)

2. Exam the cell flask under microscope to ensure the cells are healthy and check the amount of cells in each of the flasks. Choose the better one to passage.

3. Put flasks back into incubator first and get the fume hood ready for use. Spray the table surface with ethanol, wipe it with tissue. And also wipe the pipettes with ethanol.

4. Get two 10ml, one 5ml tip tubes, two new flasks and 1% Virkon (pour into a cup) and spray with ethanol before putting into the hood. Write down the cell line name, generation number, operator name, date and cell solution volume on the flasks.

5. Get the PBS and trypsin from water bath and dry with tissue. Spray and put into hood. Open the caps and loosely caped. Hand should not touch the inside of the bottle.

6. Get the chosen flask from incubator and spray before put into hood.

7. Discard the culture medium from flask into Virkon.

8. Use 10ml tip tube to get 10ml PBS. Infuse into the flask for two times, respectively (5ml each time) shake and rinse and discard to the Virkon.

9. Add 1ml trypsin with pipette into the flask and put back to incubator for 6:30 mins.

10. Get the medium from water bath, dry and spray, put into hood and unscrew the cap.

11. Use the other 10ml tip tube to get 12ml medium solution and add 6ml into each new flasks.

12. Get a new 5ml tube and spray and put into hood.

13. When 6:30 min is up, get the cell flask from incubator, shake and gently knock the bottom to detach the cells. Check under microscope to ensure most of the cells are suspended. Spray before into the hood.

14. Use the 5ml tip tube to disperse the medium by pipetting over the flask bottom up and down for 10-15 times to detach >95% the cells. Transform the cells from the flask to the 10ml tube.

15. Use pipette to add 200ul and 150ul when on Monday (or 250ul and 200ul when Friday) respectively into two new flasks. Screw back the caps and shake to make sure the cell will cover the whole bottom. Put into incubator.

16. Discard the rest of the cells into Virkon. Take the other flask of the last generation and discard into Virkon.

17. Pour the Virkon into sink and rinse with water.

18. Clean the hood and put down the window, turn off the light and turn on the UV.

A3. Schematic and parameters for the micromixer design

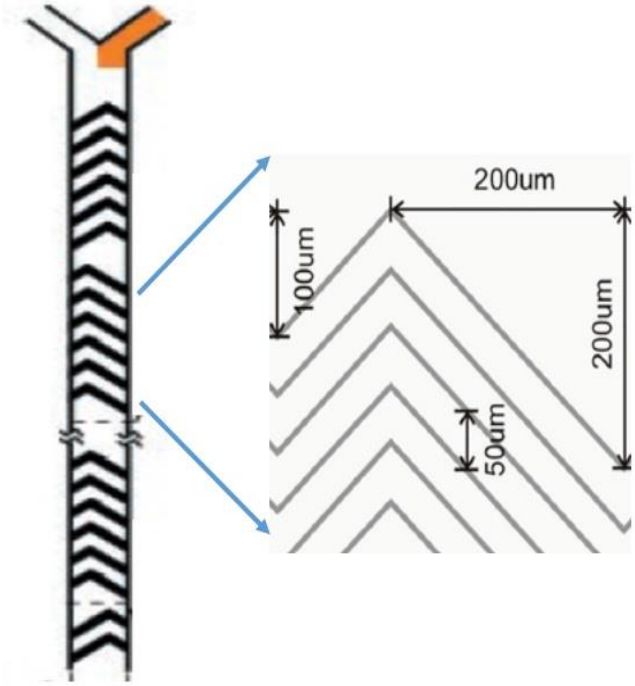

Parameters:
H=85 μm
W=300 μm
θ=45 degree
Six ridges per half-cycle

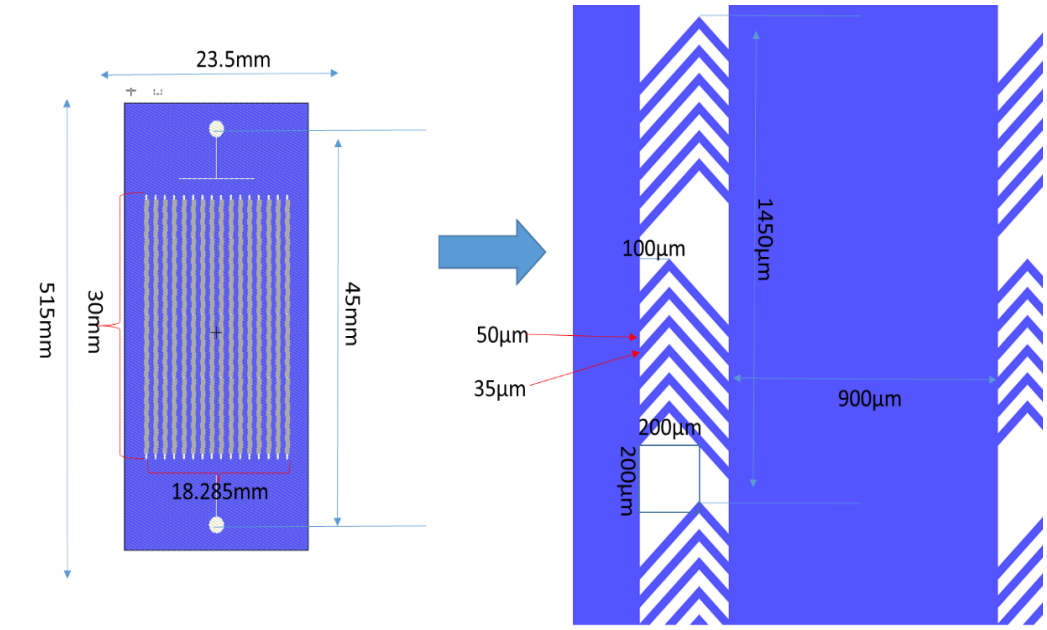

Dimension of normal cover slide is 75.6mm*24.8mm

A4. Cell clusters captured in microchannels

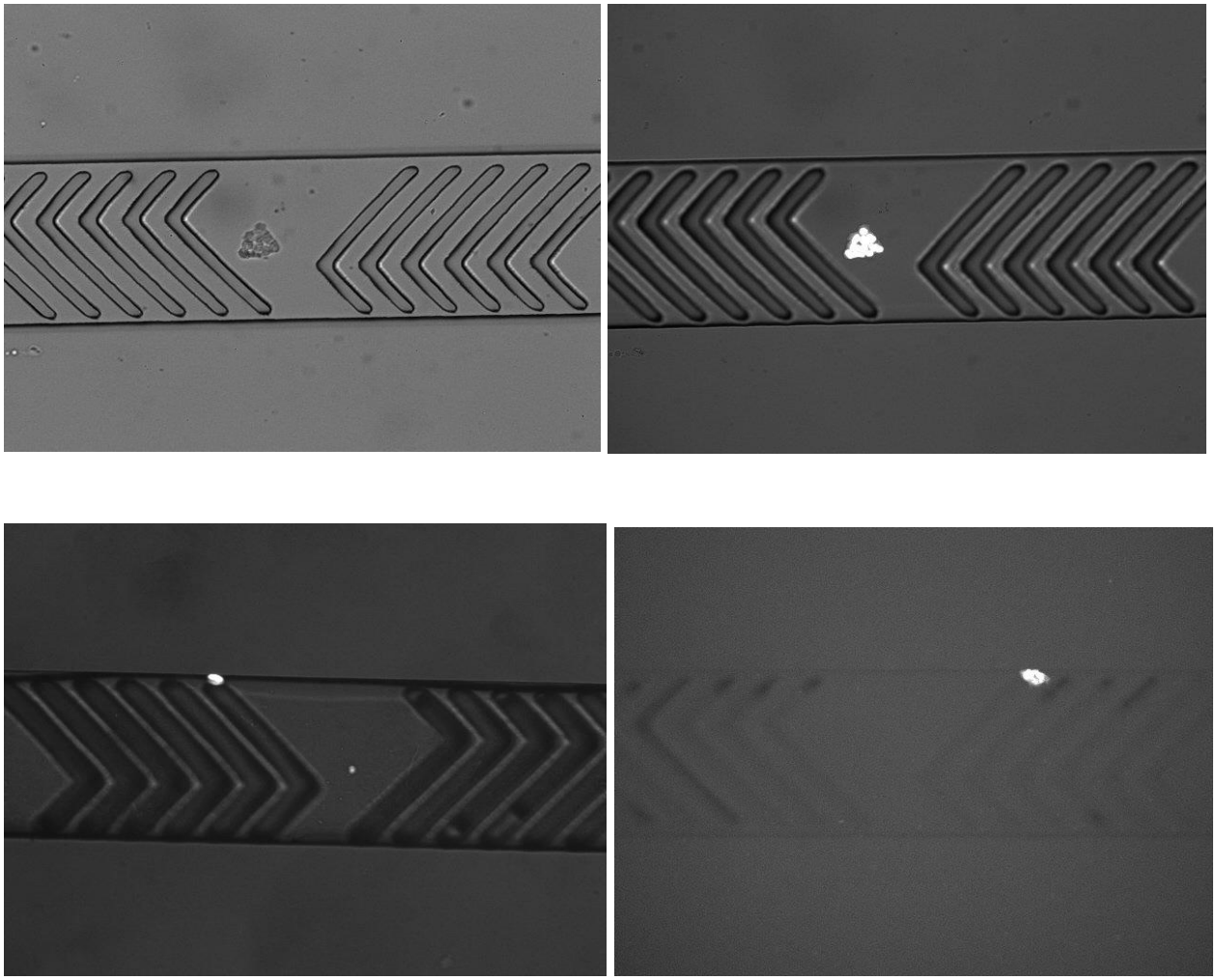

A5. Clustered cells observed in KOVA glasstic slides at higher resolution

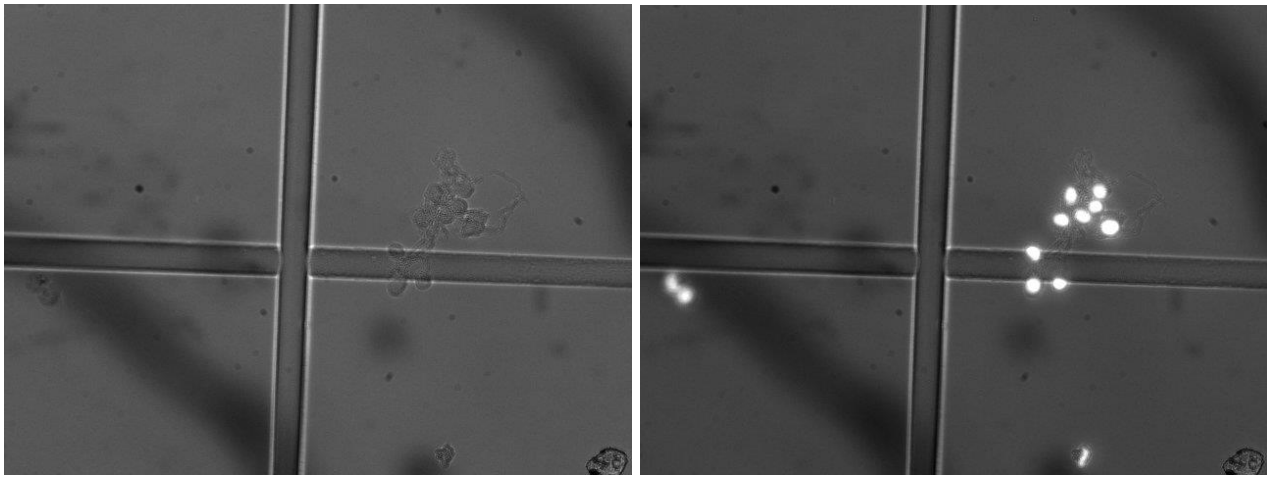

A5. Du145 and C3 Cell capture counts in GO microfluidic devices (n=5 and n=3)

Captured Cells count out of 140 cells (approx.)						
			Du145			
		Functionalized. GO Surface		Non. GO Functionalized Surface		
	GO chips	Cells Captured	Total in Percent(%)	Cells captured	Total in Percent(%)	Non GO Chips
	Chip1	82	58.57142857	51	36.42857143	I
	Chip2	95	67.85714286	39	27.85714286	II
	Chip3	73	52.14285714	57	40.71428571	III
	Chip4	86	61.42857143	49	35	IV
	Chip5	56	40	60	42.85714286	V
Average		78.4	56	51.2	36.57142857	
Standard Deviation		13.24537655	9.460983251	7.277362159	5.198115828	

	Control line	Out of 155 cells(approx.
	C3	
GO Chips	Cells Captured	Total in Percent(%)
I	25	16.12903226
II	27	17.41935484
III	17	10.96774194
		14.83870968
		2.787415354

A6. Du145 cell capture rates based on different flow rates on GO micorlfuidic devices

Cell capture vs Flow rates Data on GO functionalized Microfluidic Devices (n=1)			
Flow rates	Cells captured	Capture efficiency(%)	
3	59	42.14285714	
4	63	45	
5	60	42.85714286	
10	27	19.28571429	
20	15	10.71428571	
40	5	3.571428571	
50	3	2.142857143	

Beyond 50ul/min, cells do not have enough time to interact with bioreceptors, below 3ul/min, even flow inside the channel is difficult.

THE AMERICAN ASSOCIATION FOR THE ADVANCEMENT OF SCIENCE LICENSE TERMS AND CONDITIONS

Jul 25, 2018

This Agreement between Macquarie university -- Bhuwan Ghimire ("You") and The American Association for the Advancement of Science ("The American Association for the Advancement of Science") consists of your license details and the terms and conditions provided by The American Association for the Advancement of Science and Copyright Clearance Center.

License Number	4396181407623
License date	Jul 25, 2018
Licensed Content Publisher	The American Association for the Advancement of Science
Licensed Content Publication	Science
Licensed Content Title	Microfluidic Large-Scale Integration
Licensed Content Author	Todd Thorsen,Sebastian J. Maerkl,Stephen R. Quake
Licensed Content Date	Oct 18, 2002
Licensed Content Volume	298
Licensed Content Issue	5593
Volume number	298
Issue number	5593
Type of Use	Thesis / Dissertation
Requestor type	Scientist/individual at a research institution
Format	Electronic
Portion	Text Excerpt
Number of pages requested	1
Order reference number	
Title of your thesis / dissertation	A microfluidic device for capture and detection of circulating tumor cells
Expected completion date	Dec 2018
Estimated size(pages)	60
Requestor Location	Macquarie university Sydney Sydney, 2113 Australia Attn: Macquarie university
Billing Type	Invoice
Billing Address	Macquarie university Sydney Sydney, Australia 2113

	Attn: Macquarie university
Total	0.00 USD

Terms and Conditions

American Association for the Advancement of Science TERMS AND CONDITIONS
Regarding your request, we are pleased to grant you non-exclusive, non-transferable permission, to republish the AAAS material identified above in your work identified above, subject to the terms and conditions herein. We must be contacted for permission for any uses other than those specifically identified in your request above.
The following credit line must be printed along with the AAAS material: "From [Full Reference Citation]. Reprinted with permission from AAAS."
All required credit lines and notices must be visible any time a user accesses any part of the AAAS material and must appear on any printed copies and authorized user might make.
This permission does not apply to figures / photos / artwork or any other content or materials included in your work that are credited to non-AAAS sources. If the requested material is sourced to or references non-AAAS sources, you must obtain authorization from that source as well before using that material. You agree to hold harmless and indemnify AAAS against any claims arising from your use of any content in your work that is credited to non-AAAS sources.
If the AAAS material covered by this permission was published in Science during the years 1974 - 1994, you must also obtain permission from the author, who may grant or withhold permission, and who may or may not charge a fee if permission is granted. See original article for author's address. This condition does not apply to news articles.
The AAAS material may not be modified or altered except that figures and tables may be modified with permission from the author. Author permission for any such changes must be secured prior to your use.
Whenever possible, we ask that electronic uses of the AAAS material permitted herein include a hyperlink to the original work on AAAS's website (hyperlink may be embedded in the reference citation).
AAAS material reproduced in your work identified herein must not account for more than 30% of the total contents of that work.
AAAS must publish the full paper prior to use of any text.
AAAS material must not imply any endorsement by the American Association for the Advancement of Science.
This permission is not valid for the use of the AAAS and/or Science logos.
AAAS makes no representations or warranties as to the accuracy of any information contained in the AAAS material covered by this permission, including any warranties of merchantability or fitness for a particular purpose.
If permission fees for this use are waived, please note that AAAS reserves the right to charge for reproduction of this material in the future.
Permission is not valid unless payment is received within sixty (60) days of the issuance of this permission. If payment is not received within this time period then all rights granted herein shall be revoked and this permission will be considered null and void.
In the event of breach of any of the terms and conditions herein or any of CCC's Billing and Payment terms and conditions, all rights granted herein shall be revoked and this permission will be considered null and void.
AAAS reserves the right to terminate this permission and all rights granted herein at its

discretion, for any purpose, at any time. In the event that AAAS elects to terminate this permission, you will have no further right to publish, publicly perform, publicly display, distribute or otherwise use any matter in which the AAAS content had been included, and all fees paid hereunder shall be fully refunded to you. Notification of termination will be sent to the contact information as supplied by you during the request process and termination shall be immediate upon sending the notice. Neither AAAS nor CCC shall be liable for any costs, expenses, or damages you may incur as a result of the termination of this permission, beyond the refund noted above.

This Permission may not be amended except by written document signed by both parties.

The terms above are applicable to all permissions granted for the use of AAAS material. Below you will find additional conditions that apply to your particular type of use.

FOR A THESIS OR DISSERTATION

If you are using figure(s)/table(s), permission is granted for use in print and electronic versions of your dissertation or thesis. A full text article may be used in print versions only of a dissertation or thesis.

Permission covers the distribution of your dissertation or thesis on demand by ProQuest / UMI, provided the AAAS material covered by this permission remains in situ.

If you are an Original Author on the AAAS article being reproduced, please refer to your License to Publish for rules on reproducing your paper in a dissertation or thesis.

FOR JOURNALS:

Permission covers both print and electronic versions of your journal article, however the AAAS material may not be used in any manner other than within the context of your article.

FOR BOOKS/TEXTBOOKS:

If this license is to reuse figures/tables, then permission is granted for non-exclusive world rights in all languages in both print and electronic formats (electronic formats are defined below).

If this license is to reuse a text excerpt or a full text article, then permission is granted for non-exclusive world rights in English only. You have the option of securing either print or electronic rights or both, but electronic rights are not automatically granted and do garner additional fees. Permission for translations of text excerpts or full text articles into other languages must be obtained separately.

Licenses granted for use of AAAS material in electronic format books/textbooks are valid only in cases where the electronic version is equivalent to or substitutes for the print version of the book/textbook. The AAAS material reproduced as permitted herein must remain in situ and must not be exploited separately (for example, if permission covers the use of a full text article, the article may not be offered for access or for purchase as a stand-alone unit), except in the case of permitted textbook companions as noted below.

You must include the following notice in any electronic versions, either adjacent to the reprinted AAAS material or in the terms and conditions for use of your electronic products: "Readers may view, browse, and/or download material for temporary copying purposes only, provided these uses are for noncommercial personal purposes. Except as provided by law, this material may not be further reproduced, distributed, transmitted, modified, adapted, performed, displayed, published, or sold in whole or in part, without prior written permission from the publisher."

If your book is an academic textbook, permission covers the following companions to your textbook, provided such companions are distributed only in conjunction with your textbook at no additional cost to the user:

- Password-protected website
- Instructor's image CD/DVD and/or PowerPoint resource
- Student CD/DVD

All companions must contain instructions to users that the AAAS material may be used for non-commercial, classroom purposes only. Any other uses require the prior written permission from AAAS.

If your license is for the use of AAAS Figures/Tables, then the electronic rights granted herein permit use of the Licensed Material in any Custom Databases that you distribute the electronic versions of your textbook through, so long as the Licensed Material remains within the context of a chapter of the title identified in your request and cannot be downloaded by a user as an independent image file.

Rights also extend to copies/files of your Work (as described above) that you are required to provide for use by the visually and/or print disabled in compliance with state and federal laws.

This permission only covers a single edition of your work as identified in your request.

FOR NEWSLETTERS:

Permission covers print and/or electronic versions, provided the AAAS material reproduced as permitted herein remains in situ and is not exploited separately (for example, if permission covers the use of a full text article, the article may not be offered for access or for purchase as a stand-alone unit)

FOR ANNUAL REPORTS:

Permission covers print and electronic versions provided the AAAS material reproduced as permitted herein remains in situ and is not exploited separately (for example, if permission covers the use of a full text article, the article may not be offered for access or for purchase as a stand-alone unit)

FOR PROMOTIONAL/MARKETING USES:

Permission covers the use of AAAS material in promotional or marketing pieces such as information packets, media kits, product slide kits, brochures, or flyers limited to a single print run. The AAAS Material may not be used in any manner which implies endorsement or promotion by the American Association for the Advancement of Science (AAAS) or Science of any product or service. AAAS does not permit the reproduction of its name, logo or text on promotional literature.

If permission to use a full text article is permitted, The Science article covered by this permission must not be altered in any way. No additional printing may be set onto an article copy other than the copyright credit line required above. Any alterations must be approved in advance and in writing by AAAS. This includes, but is not limited to, the placement of sponsorship identifiers, trademarks, logos, rubber stamping or self-adhesive stickers onto the article copies.

Additionally, article copies must be a freestanding part of any information package (i.e. media kit) into which they are inserted. They may not be physically attached to anything, such as an advertising insert, or have anything attached to them, such as a sample product. Article copies must be easily removable from any kits or informational packages in which they are used. The only exception is that article copies may be inserted into three-ring binders.

FOR CORPORATE INTERNAL USE:

The AAAS material covered by this permission may not be altered in any way. No

additional printing may be set onto an article copy other than the required credit line. Any alterations must be approved in advance and in writing by AAAS. This includes, but is not limited to the placement of sponsorship identifiers, trademarks, logos, rubber stamping or self-adhesive stickers onto article copies.

If you are making article copies, copies are restricted to the number indicated in your request and must be distributed only to internal employees for internal use.

If you are using AAAS Material in Presentation Slides, the required credit line must be visible on the slide where the AAAS material will be reprinted

If you are using AAAS Material on a CD, DVD, Flash Drive, or the World Wide Web, you must include the following notice in any electronic versions, either adjacent to the reprinted AAAS material or in the terms and conditions for use of your electronic products: "Readers may view, browse, and/or download material for temporary copying purposes only, provided these uses are for noncommercial personal purposes. Except as provided by law, this material may not be further reproduced, distributed, transmitted, modified, adapted, performed, displayed, published, or sold in whole or in part, without prior written permission from the publisher." Access to any such CD, DVD, Flash Drive or Web page must be restricted to your organization's employees only.

FOR CME COURSE and SCIENTIFIC SOCIETY MEETINGS:

Permission is restricted to the particular Course, Seminar, Conference, or Meeting indicated in your request. If this license covers a text excerpt or a Full Text Article, access to the reprinted AAAS material must be restricted to attendees of your event only (if you have been granted electronic rights for use of a full text article on your website, your website must be password protected, or access restricted so that only attendees can access the content on your site).

If you are using AAAS Material on a CD, DVD, Flash Drive, or the World Wide Web, you must include the following notice in any electronic versions, either adjacent to the reprinted AAAS material or in the terms and conditions for use of your electronic products: "Readers may view, browse, and/or download material for temporary copying purposes only, provided these uses are for noncommercial personal purposes. Except as provided by law, this material may not be further reproduced, distributed, transmitted, modified, adapted, performed, displayed, published, or sold in whole or in part, without prior written permission from the publisher."

FOR POLICY REPORTS:

These rights are granted only to non-profit organizations and/or government agencies. Permission covers print and electronic versions of a report, provided the required credit line appears in both versions and provided the AAAS material reproduced as permitted herein remains in situ and is not exploited separately.

FOR CLASSROOM PHOTOCOPIES:

Permission covers distribution in print copy format only. Article copies must be freestanding and not part of a course pack. They may not be physically attached to anything or have anything attached to them.

FOR COURSEPACKS OR COURSE WEBSITES:

These rights cover use of the AAAS material in one class at one institution. Permission is valid only for a single semester after which the AAAS material must be removed from the Electronic Course website, unless new permission is obtained for an additional semester. If the material is to be distributed online, access must be restricted to students and instructors enrolled in that particular course by some means of password or access control.

FOR WEBSITES:

You must include the following notice in any electronic versions, either adjacent to the reprinted AAAS material or in the terms and conditions for use of your electronic products: "Readers may view, browse, and/or download material for temporary copying purposes only, provided these uses are for noncommercial personal purposes. Except as provided by law, this material may not be further reproduced, distributed, transmitted, modified, adapted, performed, displayed, published, or sold in whole or in part, without prior written permission from the publisher."

Permissions for the use of Full Text articles on third party websites are granted on a case by case basis and only in cases where access to the AAAS Material is restricted by some means of password or access control. Alternately, an E-Print may be purchased through our reprints department (brocheleau@rockwaterinc.com).

REGARDING FULL TEXT ARTICLE USE ON THE WORLD WIDE WEB IF YOU ARE AN 'ORIGINAL AUTHOR' OF A SCIENCE PAPER

If you chose "Original Author" as the Requestor Type, you are warranting that you are one of authors listed on the License Agreement as a "Licensed content author" or that you are acting on that author's behalf to use the Licensed content in a new work that one of the authors listed on the License Agreement as a "Licensed content author" has written.

Original Authors may post the 'Accepted Version' of their full text article on their personal or on their University website and not on any other website. The 'Accepted Version' is the version of the paper accepted for publication by AAAS including changes resulting from peer review but prior to AAAS's copy editing and production (in other words not the AAAS published version).

FOR MOVIES / FILM / TELEVISION:

Permission is granted to use, record, film, photograph, and/or tape the AAAS material in connection with your program/film and in any medium your program/film may be shown or heard, including but not limited to broadcast and cable television, radio, print, world wide web, and videocassette.

The required credit line should run in the program/film's end credits.

FOR MUSEUM EXHIBITIONS:

Permission is granted to use the AAAS material as part of a single exhibition for the duration of that exhibit. Permission for use of the material in promotional materials for the exhibit must be cleared separately with AAAS (please contact us at permissions@aaas.org).

FOR TRANSLATIONS:

Translation rights apply only to the language identified in your request summary above.

The following disclaimer must appear with your translation, on the first page of the article, after the credit line: "This translation is not an official translation by AAAS staff, nor is it endorsed by AAAS as accurate. In crucial matters, please refer to the official English-language version originally published by AAAS."

FOR USE ON A COVER:

Permission is granted to use the AAAS material on the cover of a journal issue, newsletter issue, book, textbook, or annual report in print and electronic formats provided the AAAS material reproduced as permitted herein remains in situ and is not exploited separately

By using the AAAS Material identified in your request, you agree to abide by all the terms and conditions herein.

Questions about these terms can be directed to the AAAS Permissions department permissions@aaas.org.

Other Terms and Conditions:
v 2

Questions? customercare@copyright.com or +1-855-239-3415 (toll free in the US) or +1-978-646-2777.

THE AMERICAN ASSOCIATION FOR THE ADVANCEMENT OF SCIENCE LICENSE TERMS AND CONDITIONS

Jul 25, 2018

This Agreement between Macquarie university -- Bhuwan Ghimire ("You") and The American Association for the Advancement of Science ("The American Association for the Advancement of Science") consists of your license details and the terms and conditions provided by The American Association for the Advancement of Science and Copyright Clearance Center.

License Number	4396190196605
License date	Jul 25, 2018
Licensed Content Publisher	The American Association for the Advancement of Science
Licensed Content Publication	Science
Licensed Content Title	Microfluidic Large-Scale Integration
Licensed Content Author	Todd Thorsen,Sebastian J. Maerkl,Stephen R. Quake
Licensed Content Date	Oct 18, 2002
Licensed Content Volume	298
Licensed Content Issue	5593
Volume number	298
Issue number	5593
Type of Use	Thesis / Dissertation
Requestor type	Scientist/individual at a research institution
Format	Print and electronic
Portion	Figure
Number of figures/tables	1
Order reference number	
Title of your thesis / dissertation	A microfluidic device for capture and detection of circulating tumor cells
Expected completion date	Dec 2018
Estimated size(pages)	60
Requestor Location	Macquarie university Sydney Sydney, 2113 Australia Attn: Macquarie university
Billing Type	Invoice
Billing Address	Macquarie university Sydney Sydney, Australia 2113

Attn: Macquarie university

Total 0.00 USD

Terms and Conditions

American Association for the Advancement of Science TERMS AND CONDITIONS
Regarding your request, we are pleased to grant you non-exclusive, non-transferable permission, to republish the AAAS material identified above in your work identified above, subject to the terms and conditions herein. We must be contacted for permission for any uses other than those specifically identified in your request above.
The following credit line must be printed along with the AAAS material: "From [Full Reference Citation]. Reprinted with permission from AAAS."
All required credit lines and notices must be visible any time a user accesses any part of the AAAS material and must appear on any printed copies and authorized user might make.
This permission does not apply to figures / photos / artwork or any other content or materials included in your work that are credited to non-AAAS sources. If the requested material is sourced to or references non-AAAS sources, you must obtain authorization from that source as well before using that material. You agree to hold harmless and indemnify AAAS against any claims arising from your use of any content in your work that is credited to non-AAAS sources.
If the AAAS material covered by this permission was published in Science during the years 1974 - 1994, you must also obtain permission from the author, who may grant or withhold permission, and who may or may not charge a fee if permission is granted. See original article for author's address. This condition does not apply to news articles.
The AAAS material may not be modified or altered except that figures and tables may be modified with permission from the author. Author permission for any such changes must be secured prior to your use.
Whenever possible, we ask that electronic uses of the AAAS material permitted herein include a hyperlink to the original work on AAAS's website (hyperlink may be embedded in the reference citation).
AAAS material reproduced in your work identified herein must not account for more than 30% of the total contents of that work.
AAAS must publish the full paper prior to use of any text.
AAAS material must not imply any endorsement by the American Association for the Advancement of Science.
This permission is not valid for the use of the AAAS and/or Science logos.
AAAS makes no representations or warranties as to the accuracy of any information contained in the AAAS material covered by this permission, including any warranties of merchantability or fitness for a particular purpose.
If permission fees for this use are waived, please note that AAAS reserves the right to charge for reproduction of this material in the future.
Permission is not valid unless payment is received within sixty (60) days of the issuance of this permission. If payment is not received within this time period then all rights granted herein shall be revoked and this permission will be considered null and void.
In the event of breach of any of the terms and conditions herein or any of CCC's Billing and Payment terms and conditions, all rights granted herein shall be revoked and this permission will be considered null and void.
AAAS reserves the right to terminate this permission and all rights granted herein at its

discretion, for any purpose, at any time. In the event that AAAS elects to terminate this permission, you will have no further right to publish, publicly perform, publicly display, distribute or otherwise use any matter in which the AAAS content had been included, and all fees paid hereunder shall be fully refunded to you. Notification of termination will be sent to the contact information as supplied by you during the request process and termination shall be immediate upon sending the notice. Neither AAAS nor CCC shall be liable for any costs, expenses, or damages you may incur as a result of the termination of this permission, beyond the refund noted above.

This Permission may not be amended except by written document signed by both parties.

The terms above are applicable to all permissions granted for the use of AAAS material. Below you will find additional conditions that apply to your particular type of use.

FOR A THESIS OR DISSERTATION

If you are using figure(s)/table(s), permission is granted for use in print and electronic versions of your dissertation or thesis. A full text article may be used in print versions only of a dissertation or thesis.

Permission covers the distribution of your dissertation or thesis on demand by ProQuest / UMI, provided the AAAS material covered by this permission remains in situ.

If you are an Original Author on the AAAS article being reproduced, please refer to your License to Publish for rules on reproducing your paper in a dissertation or thesis.

FOR JOURNALS:

Permission covers both print and electronic versions of your journal article, however the AAAS material may not be used in any manner other than within the context of your article.

FOR BOOKS/TEXTBOOKS:

If this license is to reuse figures/tables, then permission is granted for non-exclusive world rights in all languages in both print and electronic formats (electronic formats are defined below).

If this license is to reuse a text excerpt or a full text article, then permission is granted for non-exclusive world rights in English only. You have the option of securing either print or electronic rights or both, but electronic rights are not automatically granted and do garner additional fees. Permission for translations of text excerpts or full text articles into other languages must be obtained separately.

Licenses granted for use of AAAS material in electronic format books/textbooks are valid only in cases where the electronic version is equivalent to or substitutes for the print version of the book/textbook. The AAAS material reproduced as permitted herein must remain in situ and must not be exploited separately (for example, if permission covers the use of a full text article, the article may not be offered for access or for purchase as a stand-alone unit), except in the case of permitted textbook companions as noted below.

You must include the following notice in any electronic versions, either adjacent to the reprinted AAAS material or in the terms and conditions for use of your electronic products: "Readers may view, browse, and/or download material for temporary copying purposes only, provided these uses are for noncommercial personal purposes. Except as provided by law, this material may not be further reproduced, distributed, transmitted, modified, adapted, performed, displayed, published, or sold in whole or in part, without prior written permission from the publisher."

If your book is an academic textbook, permission covers the following companions to your textbook, provided such companions are distributed only in conjunction with your textbook at no additional cost to the user:

- Password-protected website
- Instructor's image CD/DVD and/or PowerPoint resource
- Student CD/DVD

All companions must contain instructions to users that the AAAS material may be used for non-commercial, classroom purposes only. Any other uses require the prior written permission from AAAS.

If your license is for the use of AAAS Figures/Tables, then the electronic rights granted herein permit use of the Licensed Material in any Custom Databases that you distribute the electronic versions of your textbook through, so long as the Licensed Material remains within the context of a chapter of the title identified in your request and cannot be downloaded by a user as an independent image file.

Rights also extend to copies/files of your Work (as described above) that you are required to provide for use by the visually and/or print disabled in compliance with state and federal laws.

This permission only covers a single edition of your work as identified in your request.

FOR NEWSLETTERS:

Permission covers print and/or electronic versions, provided the AAAS material reproduced as permitted herein remains in situ and is not exploited separately (for example, if permission covers the use of a full text article, the article may not be offered for access or for purchase as a stand-alone unit)

FOR ANNUAL REPORTS:

Permission covers print and electronic versions provided the AAAS material reproduced as permitted herein remains in situ and is not exploited separately (for example, if permission covers the use of a full text article, the article may not be offered for access or for purchase as a stand-alone unit)

FOR PROMOTIONAL/MARKETING USES:

Permission covers the use of AAAS material in promotional or marketing pieces such as information packets, media kits, product slide kits, brochures, or flyers limited to a single print run. The AAAS Material may not be used in any manner which implies endorsement or promotion by the American Association for the Advancement of Science (AAAS) or Science of any product or service. AAAS does not permit the reproduction of its name, logo or text on promotional literature.

If permission to use a full text article is permitted, The Science article covered by this permission must not be altered in any way. No additional printing may be set onto an article copy other than the copyright credit line required above. Any alterations must be approved in advance and in writing by AAAS. This includes, but is not limited to, the placement of sponsorship identifiers, trademarks, logos, rubber stamping or self-adhesive stickers onto the article copies.

Additionally, article copies must be a freestanding part of any information package (i.e. media kit) into which they are inserted. They may not be physically attached to anything, such as an advertising insert, or have anything attached to them, such as a sample product. Article copies must be easily removable from any kits or informational packages in which they are used. The only exception is that article copies may be inserted into three-ring binders.

FOR CORPORATE INTERNAL USE:

The AAAS material covered by this permission may not be altered in any way. No

additional printing may be set onto an article copy other than the required credit line. Any alterations must be approved in advance and in writing by AAAS. This includes, but is not limited to the placement of sponsorship identifiers, trademarks, logos, rubber stamping or self-adhesive stickers onto article copies.

If you are making article copies, copies are restricted to the number indicated in your request and must be distributed only to internal employees for internal use.

If you are using AAAS Material in Presentation Slides, the required credit line must be visible on the slide where the AAAS material will be reprinted

If you are using AAAS Material on a CD, DVD, Flash Drive, or the World Wide Web, you must include the following notice in any electronic versions, either adjacent to the reprinted AAAS material or in the terms and conditions for use of your electronic products: "Readers may view, browse, and/or download material for temporary copying purposes only, provided these uses are for noncommercial personal purposes. Except as provided by law, this material may not be further reproduced, distributed, transmitted, modified, adapted, performed, displayed, published, or sold in whole or in part, without prior written permission from the publisher." Access to any such CD, DVD, Flash Drive or Web page must be restricted to your organization's employees only.

FOR CME COURSE and SCIENTIFIC SOCIETY MEETINGS:

Permission is restricted to the particular Course, Seminar, Conference, or Meeting indicated in your request. If this license covers a text excerpt or a Full Text Article, access to the reprinted AAAS material must be restricted to attendees of your event only (if you have been granted electronic rights for use of a full text article on your website, your website must be password protected, or access restricted so that only attendees can access the content on your site).

If you are using AAAS Material on a CD, DVD, Flash Drive, or the World Wide Web, you must include the following notice in any electronic versions, either adjacent to the reprinted AAAS material or in the terms and conditions for use of your electronic products: "Readers may view, browse, and/or download material for temporary copying purposes only, provided these uses are for noncommercial personal purposes. Except as provided by law, this material may not be further reproduced, distributed, transmitted, modified, adapted, performed, displayed, published, or sold in whole or in part, without prior written permission from the publisher."

FOR POLICY REPORTS:

These rights are granted only to non-profit organizations and/or government agencies. Permission covers print and electronic versions of a report, provided the required credit line appears in both versions and provided the AAAS material reproduced as permitted herein remains in situ and is not exploited separately.

FOR CLASSROOM PHOTOCOPIES:

Permission covers distribution in print copy format only. Article copies must be freestanding and not part of a course pack. They may not be physically attached to anything or have anything attached to them.

FOR COURSEPACKS OR COURSE WEBSITES:

These rights cover use of the AAAS material in one class at one institution. Permission is valid only for a single semester after which the AAAS material must be removed from the Electronic Course website, unless new permission is obtained for an additional semester. If the material is to be distributed online, access must be restricted to students and instructors enrolled in that particular course by some means of password or access control.

FOR WEBSITES:

You must include the following notice in any electronic versions, either adjacent to the reprinted AAAS material or in the terms and conditions for use of your electronic products: "Readers may view, browse, and/or download material for temporary copying purposes only, provided these uses are for noncommercial personal purposes. Except as provided by law, this material may not be further reproduced, distributed, transmitted, modified, adapted, performed, displayed, published, or sold in whole or in part, without prior written permission from the publisher."

Permissions for the use of Full Text articles on third party websites are granted on a case by case basis and only in cases where access to the AAAS Material is restricted by some means of password or access control. Alternately, an E-Print may be purchased through our reprints department (brocheleau@rockwaterinc.com).

REGARDING FULL TEXT ARTICLE USE ON THE WORLD WIDE WEB IF YOU ARE AN 'ORIGINAL AUTHOR' OF A SCIENCE PAPER

If you chose "Original Author" as the Requestor Type, you are warranting that you are one of authors listed on the License Agreement as a "Licensed content author" or that you are acting on that author's behalf to use the Licensed content in a new work that one of the authors listed on the License Agreement as a "Licensed content author" has written.

Original Authors may post the 'Accepted Version' of their full text article on their personal or on their University website and not on any other website. The 'Accepted Version' is the version of the paper accepted for publication by AAAS including changes resulting from peer review but prior to AAAS's copy editing and production (in other words not the AAAS published version).

FOR MOVIES / FILM / TELEVISION:

Permission is granted to use, record, film, photograph, and/or tape the AAAS material in connection with your program/film and in any medium your program/film may be shown or heard, including but not limited to broadcast and cable television, radio, print, world wide web, and videocassette.

The required credit line should run in the program/film's end credits.

FOR MUSEUM EXHIBITIONS:

Permission is granted to use the AAAS material as part of a single exhibition for the duration of that exhibit. Permission for use of the material in promotional materials for the exhibit must be cleared separately with AAAS (please contact us at permissions@aaas.org).

FOR TRANSLATIONS:

Translation rights apply only to the language identified in your request summary above.

The following disclaimer must appear with your translation, on the first page of the article, after the credit line: "This translation is not an official translation by AAAS staff, nor is it endorsed by AAAS as accurate. In crucial matters, please refer to the official English-language version originally published by AAAS."

FOR USE ON A COVER:

Permission is granted to use the AAAS material on the cover of a journal issue, newsletter issue, book, textbook, or annual report in print and electronic formats provided the AAAS material reproduced as permitted herein remains in situ and is not exploited separately

By using the AAAS Material identified in your request, you agree to abide by all the terms and conditions herein.

Questions about these terms can be directed to the AAAS Permissions department permissions@aaas.org.

Other Terms and Conditions:
v 2

Questions? customercare@copyright.com or +1-855-239-3415 (toll free in the US) or +1-978-646-2777.

SPRINGER NATURE LICENSE TERMS AND CONDITIONS

Oct 10, 2018

This Agreement between Bhuwan Ghimire ("You") and Springer Nature ("Springer Nature") consists of your license details and the terms and conditions provided by Springer Nature and Copyright Clearance Center.

License Number	4445160072135
License date	Oct 10, 2018
Licensed Content Publisher	Springer Nature
Licensed Content Publication	Springer eBook
Licensed Content Title	Non-Newtonian Fluids: An Introduction
Licensed Content Author	Rajendra P. Chhabra
Licensed Content Date	Jan 1, 2010
Type of Use	Thesis/Dissertation
Requestor type	academic/university or research institute
Format	print and electronic
Portion	figures/tables/illustrations
Number of figures/tables /illustrations	1
Will you be translating?	no
Circulation/distribution	<501
Author of this Springer Nature content	no
Title	Isolation of cancer cells on nanomaterial functionalized microfluidic devices
Instructor name	Prof. Jim Piper
Institution name	Macquarie University
Expected presentation date	Oct 2018
Portions	Figure 1.4
Requestor Location	Bhuwan Ghimire 6/9 cottonwood crescent macquarie park Sydney, other 2113 Australia Attn:
Billing Type	Invoice
Billing Address	Bhuwan Ghimire 6/9 cottonwood crescent macquarie park Sydney, Australia 2113 Attn: Bhuwan Ghimire
Total	0.00 USD

Terms and Conditions

Springer Nature Terms and Conditions for RightsLink Permissions

Springer Nature Customer Service Centre GmbH (the Licensor) hereby grants you a non-exclusive, world-wide licence to reproduce the material and for the purpose and requirements specified in the attached copy of your order form, and for no other use, subject to the conditions below:

1. The Licensor warrants that it has, to the best of its knowledge, the rights to license reuse of this material. However, you should ensure that the material you are requesting is original to the Licensor and does not carry the copyright of another entity (as credited in the published version).

   If the credit line on any part of the material you have requested indicates that it was reprinted or adapted with permission from another source, then you should also seek permission from that source to reuse the material.

2. Where **print only** permission has been granted for a fee, separate permission must be obtained for any additional electronic re-use.

3. Permission granted **free of charge** for material in print is also usually granted for any electronic version of that work, provided that the material is incidental to your work as a whole and that the electronic version is essentially equivalent to, or substitutes for, the print version.

4. A licence for 'post on a website' is valid for 12 months from the licence date. This licence does not cover use of full text articles on websites.

5. Where **'reuse in a dissertation/thesis'** has been selected the following terms apply: Print rights of the final author's accepted manuscript (for clarity, NOT the published version) for up to 100 copies, electronic rights for use only on a personal website or institutional repository as defined by the Sherpa guideline (www.sherpa.ac.uk/romeo/).

6. Permission granted for books and journals is granted for the lifetime of the first edition and does not apply to second and subsequent editions (except where the first edition permission was granted free of charge or for signatories to the STM Permissions Guidelines http://www.stm-assoc.org/copyright-legal-affairs/permissions/permissions-guidelines/), and does not apply for editions in other languages unless additional translation rights have been granted separately in the licence.

7. Rights for additional components such as custom editions and derivatives require additional permission and may be subject to an additional fee. Please apply to Journalpermissions@springernature.com/bookpermissions@springernature.com for these rights.

8. The Licensor's permission must be acknowledged next to the licensed material in print. In electronic form, this acknowledgement must be visible at the same time as the figures/tables/illustrations or abstract, and must be hyperlinked to the journal/book's homepage. Our required acknowledgement format is in the Appendix below.

9. Use of the material for incidental promotional use, minor editing privileges (this does not include cropping, adapting, omitting material or any other changes that affect the meaning, intention or moral rights of the author) and copies for the disabled are permitted under this licence.

10. Minor adaptations of single figures (changes of format, colour and style) do not require the Licensor's approval. However, the adaptation should be credited as shown in Appendix below.

Appendix — Acknowledgements:

For Journal Content:
Reprinted by permission from [**the Licensor**]: [**Journal Publisher** (e.g. Nature/Springer/Palgrave)] [**JOURNAL NAME**] [**REFERENCE CITATION** (Article name, Author(s) Name), [**COPYRIGHT**] (year of publication)

For **Advance Online Publication papers:**
Reprinted by permission from [**the Licensor**]: [**Journal Publisher** (e.g. Nature/Springer/Palgrave)] [**JOURNAL NAME**] [**REFERENCE CITATION** (Article name, Author(s) Name), [**COPYRIGHT**] (year of publication), advance online publication, day month year (doi: 10.1038/sj.[JOURNAL ACRONYM].)

For Adaptations/Translations:
Adapted/Translated by permission from [**the Licensor**]: [**Journal Publisher** (e.g. Nature/Springer/Palgrave)] [**JOURNAL NAME**] [**REFERENCE CITATION** (Article name, Author(s) Name), [**COPYRIGHT**] (year of publication)

Note: For any republication from the British Journal of Cancer, the following credit line style applies:

Reprinted/adapted/translated by permission from [**the Licensor**]: on behalf of Cancer Research UK: : [**Journal Publisher** (e.g. Nature/Springer/Palgrave)] [**JOURNAL NAME**] [**REFERENCE CITATION** (Article name, Author(s) Name), [**COPYRIGHT]** (year of publication)

For **Advance Online Publication** papers:
Reprinted by permission from The [**the Licensor**]: on behalf of Cancer Research UK: [**Journal Publisher** (e.g. Nature/Springer/Palgrave)] [**JOURNAL NAME**] [**REFERENCE CITATION** (Article name, Author(s) Name), [**COPYRIGHT**] (year of publication), advance online publication, day month year (doi: 10.1038/sj.[JOURNAL ACRONYM])

For Book content:
Reprinted/adapted by permission from [**the Licensor**]: [**Book Publisher** (e.g. Palgrave Macmillan, Springer etc) [**Book Title**] by [**Book author**(s)] [**COPYRIGHT**] (year of publication)

Other Conditions:

Version 1.1